Final Report

ANALYSIS OF MINUTEMAN EXHAUST PRODUCTS

Prepared for:

AEROJET-GENERAL CORPORATION
NIMBUS, CALIFORNIA

PURCHASE ORDER NO. S507323-OP
UNDER CONTRACT AF 33(600)36610

STANFORD RESEARCH INSTITUTE
MENLO PARK, CALIFORNIA

SRI

October 25, 1962

Final Report

ANALYSIS OF MINUTEMAN EXHAUST PRODUCTS

Prepared for:

AEROJET-GENERAL CORPORATION
NIMBUS, CALIFORNIA

PURCHASE ORDER NO. S607323-OP
UNDER CONTRACT AF 33(600)36610

By: *Eugene A. Burns*

SRI Project No. PRD-3753

Approved:

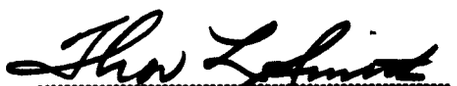

THOR L. SMITH, DIRECTOR
PROPULSION SCIENCES DIVISION

Copy No. 10

CONTENTS

CONTENTS (concluded)

ILLUSTRATIONS

ILLUSTRATIONS (continued)

ILLUSTRATIONS (concluded)

TABLES

TABLES (concluded)

I INTRODUCTION

At the present time it is possible to calculate the theoretical specific impulse of Minuteman propellants with a high degree of accuracy. The delivered specific impulse falls considerably short of the calculated value, however, and it is important to determine quantitatively the relative contribution of the factors responsible for this discrepancy such as combustion efficiency, thermal lags, particle lag, and lack of approach to chemical equilibrium.

Knowledge of the chemical composition of Minuteman exhaust products would permit the determination of combustion efficiency and lack of approach to chemical equilibrium. There have been many attempts in the past to sample rocket exhaust products and to determine the composition existing at some point in the exhaust stream; although the difficulties encountered are widely recognized, the advantages offered by modern analytical techniques have not been realized up to this time.

In addition to improved analytical techniques, it should be possible to devise better sampling techniques than are now available. The current practice of sampling the exhaust products at a distance from the nozzle is faulty, because the species which have not attained complete combustion at the throat continue to react in the exhaust of the rocket.[1] Some investigators have permitted the combustion products to expand into a chamber which contains an inert gas.[2] The inert atmosphere utilized by these workers may appear at first to be sound in principle, but upon reflection one may perceive that the exhaust gases collected in the chamber are not inert; the oxidizing products present in the gases are more than sufficient to attack any aluminum which is not oxidized by the time it is at the nozzle throat and expansion section.

Current researchers have also failed to utilize modern analytical chemistry techniques to the fullest extent. Combustion products which are gases at ambient temperature have been examined by Orsat

techniques, gas-liquid partition chromatography, and infrared spectrometry, but not by the much more discriminating tool, mass spectrometry. Exhaust products which are solids at room temperatures have been examined by X-ray diffraction, metallographic analysis, and chemical analysis. Most chemical analyses will not distinguish between metallic aluminum and alumina, or aluminum suboxides.

As a result of discussions with cognizant individuals at Aerojet-General Corporation, a subcontract was let to Stanford Research Institute with the objective of developing the necessary analytical techniques and sampling techniques to give a more accurate estimation of the chemical composition of Minuteman exhaust products at well-defined points in the expansion zone. Upon development of these analytical techniques direct measurements during motor firings were to be made so that the results would be available for interpretation and comparison with theoretical calculations.

The Minuteman-type propellant (ammonium perchlorate-polyurethane propellants containing aluminum) creates an array of combustion products, which are predominantly hydrogen, carbon monoxide, hydrogen chloride, aluminum oxide, and nitrogen. Other species likely to be present are carbon, aluminum, aluminum suboxides, aluminum carbides, aluminum oxycarbides, aluminum chlorides, and carbon dioxide. It has been reported[3-5] that the equilibria existing among the vapor species Al, Al_2O, AlO, and Al_2O_3 depend upon the temperature and whether the ambient atmosphere is reducing or neutral. Upon slow cooling, only stable Al or Al_2O_3 molecules would be obtained; however, if the sample vapors are quenched rapidly with an efficient heat exchanger, it is anticipated that Al_2O and/or AlO may be frozen <u>in situ</u>. In this way the existence of such recognized species as Al_4O_4C and Al_4C_3 in the exhaust may be established; these products most likely arise upon cooling rather than existing at the combustion temperature. On the contrary, it has been reported that it is not possible to quench the reduced aluminum oxide vapors without disproportionation to aluminum and alumina.[6] Mass spectrometric studies[7] show that at elevated temperatures the predominant carbide of aluminum volatilized is Al_2C_2 rather than previously reported Al_4C_3.

II SUMMARY

Analytical methods based primarily on infrared spectroscopy, gas-solid partition chromatography, and mass spectroscopy have been developed for the compositional determination of trapped rocket exhaust gases; the validity of the methods was established by analysis of synthetic mixtures of typical exhaust gases.

Analytical methods have also been devised for the compositional analysis of trapped solid exhaust products; these methods have been checked by analysis of synthetic mixtures.

A technique for trapping the exhaust products in the vicinity of the exit plane has been developed. A probe (protected from melting by tantalum shielding) is swept through the exhaust with a rotational motion such that exhaust products can be trapped at some pre-selected point; the point can be varied from within the nozzle to any desired point downstream. By use of a double chamber in the probe, along with appropriate vacuum techniques, samples of both solid and gaseous components can be trapped which are free from contamination by other gases such as air.

The exhaust sampling technique was evaluated by sampling 5-lb, 5 x 7 inch tubular rocket motors containing aluminized polyurethane propellants. The technique was perfected in the course of sampling exhausts of Aerojet-General's 3KS-1000 rocket motors containing Minuteman-type propellant at Nimbus, California.

The solid exhaust products collected at the exit plane were black and porous with some patches of gold; a few inches from the exit plane, the exhaust products were white.

Quantitative data are given to show that:

1. Complete combustion of aluminum does not take place before the sample is trapped at the exit plane of the nozzle.

2. Combustion continues in the exhaust stream, although a few inches from the exit plane it is essentially complete.

3. Increased chamber pressure decreases the concentration of unburned aluminum.

4. The degree of combustion is enhanced as the ammonium perchlorate-to-aluminum ratio is increased.

5. Increased residence time in the combustion chamber increases the degree of combustion.

III DEVELOPMENT OF ANALYTICAL METHODS

Development of new analytical methods and evaluation of the applicability of existing methods for the analysis of both gaseous and solid exhaust products was a necessary requirement for the successful completion of this work. The methods developed were checked for applicability by analysis of synthetic mixtures of known concentration. These methods are categorized below as analysis of either gaseous or solid mixtures.

A. Analysis of Synthetic Gas Mixtures

The exhaust gases from the combustion of an aluminized polyurethane propellant as predicted by thermodynamic calculation are hydrogen chloride, nitrogen, hydrogen, carbon monoxide, water, and carbon dioxide. When the gases have cooled to room temperature and the pressure reduced, some trapped water will condense in the probes of the size used in the exhaust samplings. To complicate matters, the affinity of hydrogen chloride for water is so great that appreciable quantities of HCl will be absorbed in the water. Because of the reduced pressure and the hydrogen chloride concentration a negligible amount of carbon dioxide will be absorbed by the water. To obviate difficulties resulting from the water and hydrogen chloride, the gas sample is passed over a cold pyridine slush to absorb the water and hydrogen chloride, and hence these need not be of concern in subsequent determinations. Determination of the carbon dioxide-carbon monoxide ratio by infrared spectroscopy is not affected by hydrogen chloride and this ratio was determined in its presence; the actual percentage of carbon dioxide and carbon monoxide was calculated on a HCl-free basis. Synthetic mixtures of gases were prepared in an all-glass gas handling device which permitted known amounts of the gas in question to be metered into a large bulb and measured with manometric accuracy.

1. Infrared Analysis

The infrared spectra of synthetic mixtures of hydrogen chloride, carbon dioxide, carbon monoxide, nitrogen, and hydrogen were examined and calibration curves for the absorbance at 2940 cm^{-1} and 2820 cm^{-1} for hydrogen chloride, 2355 cm^{-1} and 2340 cm^{-1} for carbon dioxide, and 2170 cm^{-1} and 2120 cm^{-1} for carbon monoxide were determined. Details of this method as well as typical calibration curves and a statistical evaluation of the method for determining the CO_2 /CO ratio in synthetic mixtures are presented in Appendix A.

2. Gas-Solid Partition Chromatographic Analysis

The analysis of synthetic gas mixtures by gas-solid partition chromatography was accomplished by introduction of the sample into a Wilkins Instrument Company gas chromatograph by means of a Beckman Instrument Company gas sampling valve. A slow leak exists in this valve but a correction is easily applied for the small amount of air introduced while filling the sampling loop. A 10-foot-long, 1/4-inch-diameter, Molecular Sieve 13X column is used to separate hydrogen, nitrogen, and carbon monoxide. Carbon dioxide is totally absorbed at ambient temperatures. Oxygen is also separated, and from its area the correction for the air leak is calculated and then applied to the nitrogen peak. Carbon dioxide is separated from the other components on a silica gel column; however, the sensitivity of this partition is poor. Because the carbon dioxide level in the exhaust sample is low and because the pressure of the sample is only about half an atmosphere, the precision suffers. The necessary area x time determination was accomplished using a Disc integrator. Experimental details of this method are given in Appendix B.

3. Mass Spectrometric Analysis

Mass spectrometric cracking patterns of the gases expected in Minuteman exhausts were evaluated and sensitivity factors determined. Hydrogen chloride was not examined because of its known detrimental effect on the stainless steel sampling system. Details of the calculation of the composition from the cracking pattern are presented as Appendix C.

B. Analysis of Synthetic Solid Mixtures

The expected composition of the solid matter trapped from Minuteman-type rocket exhausts should principally consist of aluminum oxide, aluminum carbide, aluminum, water, and carbon. Aluminum suboxides and oxycarbides could also be present, as products of the combustion and/or reaction of the hot gases and particles with the nozzle walls. Impurities which stem from the walls and tip of the probe itself that are likely to be present in the solid product are ferric oxide and tantalic oxide. The following methods were developed and tested for applicability by analyzing synthetic mixtures of the typical solid products outlined above.

1. Determination of Metallic Aluminum in Aluminum-Alumina Mixtures

The determination of metallic aluminum and/or reduced oxides of aluminum in the presence of alumina has been accomplished in the past eudiometrically.[8,9] This method is based upon measurement of hydrogen gas evolved by action of sodium hydroxide with metallic aluminum. The eudiometric method is not applicable to rocket exhaust products because, upon cooling, the unburned aluminum in the exhaust is encapsulated by a refractory coating of alumina, and this coating is impervious to the action of sodium hydroxide.

The method developed here avoids the coating difficulty by dissolution of the sample in a pyrophosphate melt simultaneously with combustion of the metallic aluminum in a controlled-oxygen atmosphere. Suitable corrections are applied for carbon dioxide and water emanating from the combustion boat, which contains the sample and flux. The net weight increase of the combustion boat represents the quantity of oxygen that combined with the metallic aluminum, e.g.,

$$4Al + 3O_2 \longrightarrow 2Al_2O_3 \qquad (3)$$

$$C + O_2 \longrightarrow CO_2 \uparrow \qquad (4)$$

Hence, this method provides the determination of carbon, water, and metallic aluminum; it has a standard deviation of 0.08% Al in the range 0-10% Al. Details of the method are found in Appendix D.

2. Solution of Refractory Alumina-Aluminum Mixtures

Solution of alumina-aluminum refractory mixtures is required prior to the determination of aluminum described above. Several standard fluxes for the fusion of this refractory were examined. Fusion with sodium carbonate was not easily effected; however, satisfactory fusion with potassium bisulfate was obtained. The detailed procedure is presented in Appendix E.

3. Determination of Aluminum

For the complete analysis of the solid exhaust products, an accurate analytical method was required for the determination of total aluminum. Several standard methods were surveyed; because of the relative small size of exhaust sample to be collected, a volumetric method was chosen over gravimetric methods. Several volumetric methods were tested, and one similar to that proposed by Wannainen and Ringbom[10] was selected. The method consists of reaction of aluminum with an excess of disodium ethylenediaminetetraacetate solution (EDTA) of known strength (Eq. 1)

$$Al^{+++} + H_2Y^{=} \longrightarrow AlY^{-} + 2H^{+} \qquad (1)$$

$$H_2Y^{=} + Zn^{++} \longrightarrow ZnY^{=} + 2H^{+} \qquad (2)$$

and back titration, in a buffered 50% ethanol, with standard zinc acetate solution (Eq. 2) using dithizone as internal indicator. The exact procedure and typical results are given in Appendix F. The coefficient of variation of this method is 0.48% at a concentration level of 0.6 mmole, and 0.68% at a level of 0.06 mmole.

4. Determination of Iron

Iron is introduced into the solid exhaust product by action of the exhaust on the Teflon-coated stainless steel walls of the probe. Its determination is accomplished polarographically after solution of the sample by sulfate-bisulfate fusion.[11] Specific details of this method are found in Appendix G.

5. Determination of Titanium

It is difficult to conceive how titanium could be present in the solid exhaust product. However when X-ray diffraction studies indicated that it may be present, a spectrophotometric method[12] based on formation of the peroxytitanic complex ion (Eq. 5) was evaluated for its applicability in a typical fusion mixture:

$$TiO + H_2O_2 + H_2O \longrightarrow TiO_4^{=} + 4H^{+} \qquad (5)$$

This method proved that titanium was not present in the exhaust. Details of this method are located in Appendix H.

6. Determination of Tantalum

Tantalum originated in the exhaust product by ablation from the probe tip. Two different methods for determining the Ta content were employed in this work. The first method[13] is based upon formation of the peroxytantalic complex ion $TaO_4^{=}$ (Eq. 6)

$$2TaF_6^{\equiv} + H_2O_2 + 6H_2O + 2H^{+} \longrightarrow 2TaO_4^{=} + 16HF \qquad (6)$$

and measurement [12] of its absorbance at 286 mμ. This method was evaluated and found to be applicable if extreme care is taken in the preparation of the peroxytantalic complex ion, for it is subject to destruction with small amounts of impurities. Details of this method can be found in Appendix I.

Because of the tedious nature of the peroxy determination, a recently reported spectrophotometric method[14] was evaluated to ascertain whether it had sufficient advantages to be used in the subsequent tantalum determinations. This method is based upon conversion of a solution of tantalum fluoride to its methyl violet complex; subsequent partition from the bulk of the solution by extraction with toluene; and finally measurement of the absorbance of the solution at 605 mμ. The method was tested and with suitable modifications was found to be applicable to the analysis of the solid exhaust products. This method is recommended rather than the peroxide spectrophotometric method, for the following reasons:

1. Preparation of the sample is easier.
2. It is on sounder theoretical ground because the reference solution does not absorb significantly.
3. It is 25 times more sensitive.
4. Adjustment of the concentration of the reactants is not as critical.
5. A correction for the amount of iron in the sample is not necessary.

The detailed description of the method is found in Appendix J.

IV EXHAUST PRODUCT SAMPLING METHODOLOGY

The trapping technique consisted of inserting a probe into the exhaust stream for a finite interval (during which a sample is obtained) and then removing the probe and contents before thermal destruction. The development of the apparatus and sampling technique is presented chronologically in this section.

A. Initial Probe Configuration

The initial probe used in this work is shown disassembled in Fig. 1. Figures 2a and 2b show the assembled probe, together with its hydraulic actuator, in three orientations of its motion as it travels through the rocket exhaust. Drawings of the probe and track are in Appendix K. The probe was fabricated from stainless steel, and the inner surfaces were coated with Teflon to eliminate reaction of the hot hydrogen chloride with the probe surfaces. The probe was completely surrounded by a 1/4-inch-thick chamber in which a coolant could be maintained. The inlet and outlet for the coolant are the two bent 1/4-inch-diameter stainless tubes shown projecting from the rear of the probe in Fig. 1. Because of the supersonic velocities of the exhaust products, material will only be trapped by the traversing probe when the probe is parallel with the axis of the rocket exhaust. Check valves were installed at the exit and entrance of the probe so that a vacuum can be maintained in the chamber prior to use and a maximum pressure of 30 psia can be held in the chamber. By proper adjustment of the velocity of the probe, it was possible to minimize the duration of the probe in the rocket exhaust, yet permit a sample at a pressure of 30 psia to be collected. The apparatus was equipped with a pressure transducer so that the times at which trapping begins and ends can be recorded.

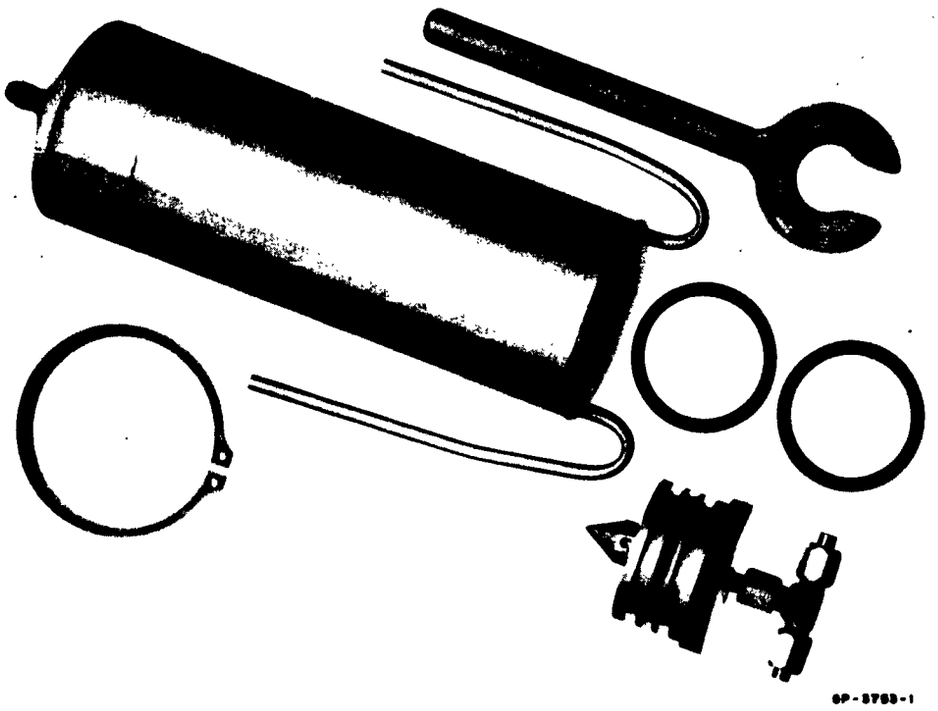

FIG. 1 DISASSEMBLED ROCKET EXHAUST SAMPLING PROBE

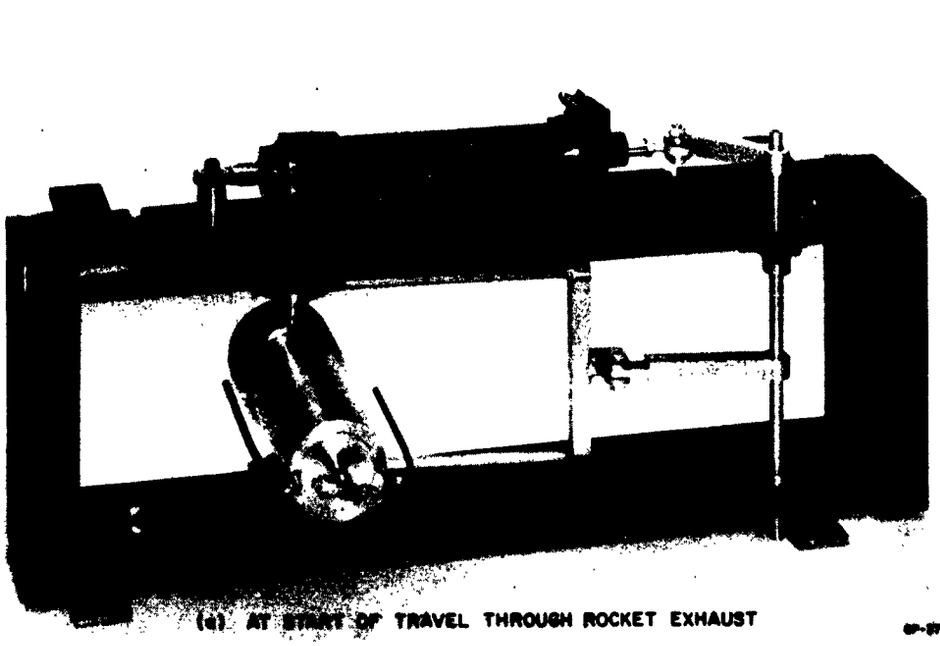

(a) AT START OF TRAVEL THROUGH ROCKET EXHAUST

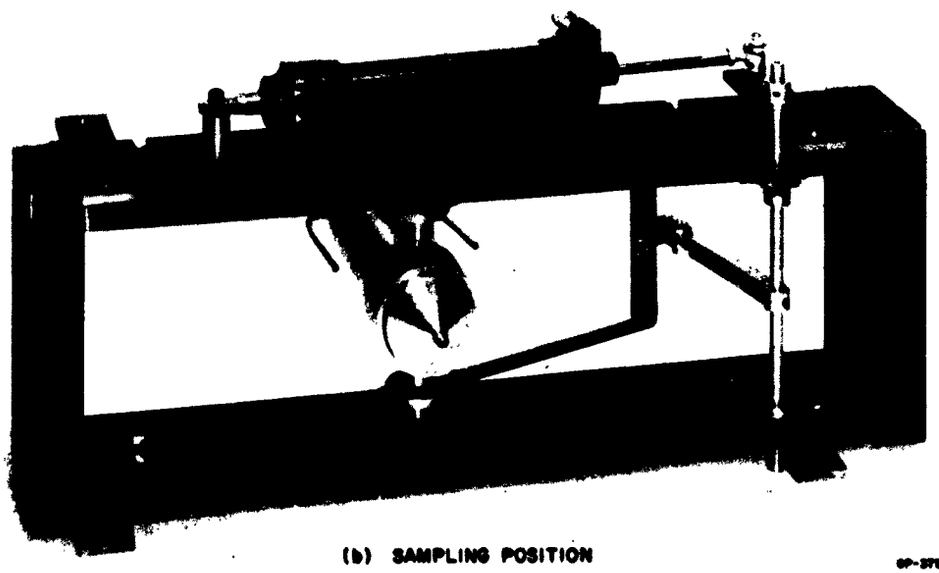

(b) SAMPLING POSITION

FIG. 2 HYDRAULIC ACTUATOR AND PROBE IN VARIOUS ORIENTATIONS
(a) at start of travel through rocket exhaust
(b) sampling position

After trapping, the gases were transferred to a standard gas-handling bulb, and the solid material was scraped out and retained for subsequent analysis. The actuation circuits and transducers for the probe were found to be satisfactory when tested as follows. Four cylinders of nitrogen gas were attached via a manifold to a rocket case and were allowed to expand through a 1/4-inch nozzle. The chamber pressure reached 600 psi and the gas expanding through the nozzle attained a supersonic velocity. Two seconds after opening the manifold line valve a steady-state condition developed, and about one second later the probe was actuated. The velocity of the probe was controlled so that the complete travel required 1.0 second. The history of the chamber pressure, probe pressure, and position indicator is shown in Fig. 3. As anticipated, trapping did not occur until the probe was in the center of its travel, i.e., in the axis of the exhaust. However, trapping continued for about 0.3 second; the maximum pressure (45 psi) developed in the probe 0.15 second after it reached the axis of the exhaust. The pressure in probe dropped to 2 psi as the check valve used for this test was a 2-psi check valve instead of the 20-psi valve used later.

B. Rocket Motors

For most of the work the exhaust of Aerojet-General's ANP-2699 aluminized-polyurethane propellant was sampled. This propellant was chosen for two reasons: (1) the high aluminum content (17%) optimized the concentration of any non-oxidized aluminum emanating from the nozzle, and (2) numerous calculations concerning the theoretical composition of the exhaust were already available[15] thus permitting, if desired, a meaningful comparison to be made between theoretical and experimental facts. Five-pound tubular non-restricted grains with a web thickness of 1.25 inches were cast into 5x7-inch motor cases. The burning rate of this propellant (measured by strand burning) is 0.31 in/sec at 1000 psi. With the particular nozzle configuration used, it was anticipated that a maximum chamber pressure of about 630 psi would be realized and that the duration of burning would be about 4.5 seconds.

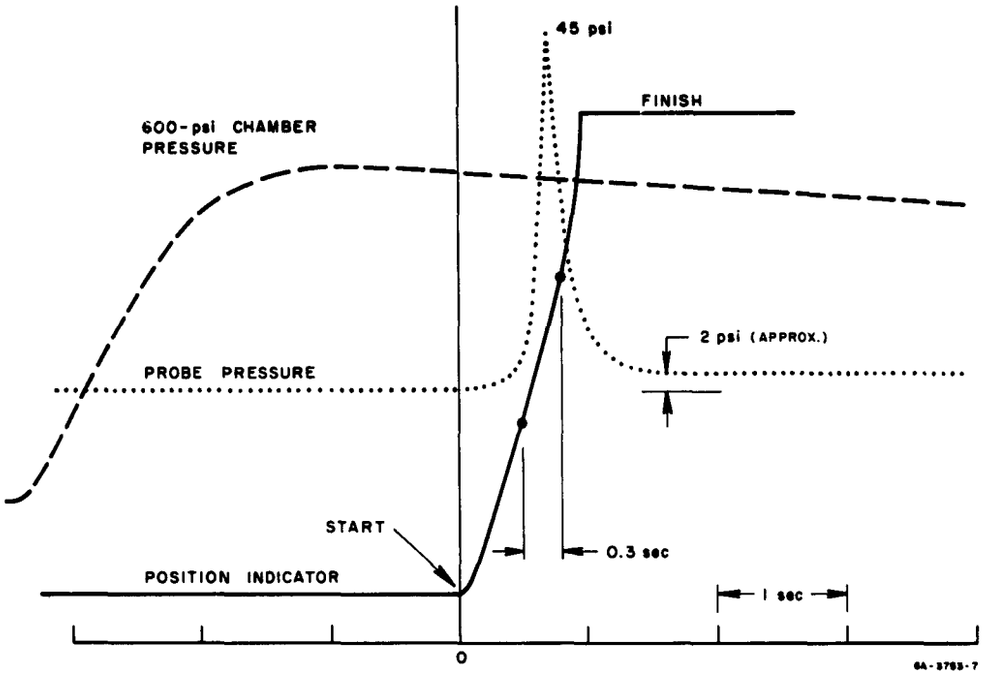

FIG. 3 CHAMBER PRESSURE, PROBE PRESSURE, AND POSITION INDICATOR AS A FUNCTION OF TIME OF NITROGEN TEST (see test for details)

The only exception to the motors described above was the first one which was loaded with a typical JPL-type aluminum-ammonium perchlorate-polyurethane propellant containing 3% copper chromate as a burning rate additive. This propellant had a high burning rate, and for the 5x7 inch engine employed, the motor had a burning time of 2.2 seconds.

C. Evaluation of Operating Parameters

The major operating parameters for the sampling are listed in Table I. These parameters are explained below with the significant findings of each experiment. The direction of the work was towards the successful trapping of a significant quantity of solid exhaust product and containment of the gaseous products. Some of the findings of these experiments are summarized in Table II. It was desired to give the

Table I

SUMMARY OF EXHAUST SAMPLING PARAMETERS

Run	Distance from exhaust plane at 180° position (inch)	Time from ignition to activation of probe (sec)	Lag in motion of probe (sec)	Sweep Time			Total firing time (sec)
				Total (sec)	90° to 270° (sec)	Time from ignition to 180° (sec)	
A	0.13[a]	- - -	- - -	- - -	- - -	- - -	2.28
1	0.13[b]	- - -	- - -	- - -	- - -	1.92	4.54
2	0.13[b]	- - -	- - -	- - -	- - -	- - -	4.53
3	0.13[b]	- - -	- - -	1.16	0.39	1.97	4.57
4	0.13[b]	- - -	- - -	1.91	0.53	2.00	4.51
5	0.13[b, c]	- - -	- - -	2.14	0.59	2.33	4.65
6	0.19	0.93	0.28	2.32	0.58	2.95	4.57
7	0.19[c]	0.85	0.23	2.36	0.66	2.40	4.53
8	0.19	0.96	0.25	1.88	0.58	2.66	4.68
9	0.19	0.78	0.28	1.95	0.61	2.59	4.68
10	1.56	0.95	0.21	1.97	0.63	2.72	4.79
11	1.56	0.92	0.24	1.97	0.57	2.72	4.68
12	0.19	0.76	0.30	2.06	0.69	2.54	4.60
13	0.19	0.79	0.19	2.03	0.65	2.67	4.67
14	-0.25	0.82	0.27	2.13	0.93	2.77	4.67
15	0.19	0.70	0.36	1.90	0.76	2.55	4.61
16	1.50	0.73	0.29	2.09	0.71	2.69	4.48
17	-0.25	0.73	0.29	2.07	0.82	2.59	4.78
18	0.50	0.60	0.28	2.01	0.70	2.42	4.75
19	-0.25	0.69	0.31	1.96	0.75	2.50	4.71

a - 1/4" stainless steel probe tip , b - 1-1/4" tantalum tip with 0.19 inch bore

c - Tip bore beveled at 45° to depth of .13 inch

Table II

RESULTS OF EXHAUST SAMPLING EXPERIMENTS

Run	Solid matter trapped (g)	Chamber pressure at 180° position (psig)	Nozzle pressure at 180° position (atm.)	ΔP_A [a] (psi)	Max. probe pressure (psig)	Gases contained (atm.)
A	- -	- -	- -	- -	- -	
1	- -	638	0.56	- -	17	
2	0.10	- -	- -	- -	- -	
3	0.26	623	0.52	- -	- -	1.0
4	0.47	622	0.64	- -	57	1.0
5	1.05	586	0.64	- -	78	1.0
6	1.26	528	- -	65	72	1.0
7	1.48	588	0.63	61	76	1.0
8	2.15	530	0.66	56	95	1.0
9	2.10	552	0.67	60	- -	1.0
10	1.29	552	0.65	42	41	1.0
11	1.46	560	0.64	44	37	1.0
12	2.07	566	0.65	55	50	2.2
13	1.97	531	0.72	64	52	2.2
14	3.13	544	- -	53	68	2.7
15	2.87	691	- -	53	40	2.7
16	1.12	680	0.64	54	37	1.2
17	2.93	- -	2.14	48	40	1.0
18	2.35	556	0.65	51	33	2.3
19	2.62	540	2.33	48	38	2.4

[a] ΔP_A is the pressure differential in the hydraulic actuator required to drive the probe through the exhaust after the probe hesitates on initial contact with the exhaust stream.

probe a rigorous test--by being in a trapping position for 0.5 sec--thus requiring control of the total sweep interval. The rate of sweep of the probe through the exhaust was controlled by adjustment of the pressure differential which actuates the hydraulic drive piston. When a 0.5-sec trapping position requirement is met--in the absence of a rocket exhaust--the probe is out of the trapping position at 2.1 sec after actuation and has a total sweep time of 3.4 sec. Because of the short burning time, actuation of the probe sweep was commenced 0.2 sec before ignition so that the probe would be through trapping before burning ceased. However, with the hydraulic setup employed, the probe was held up by the exhaust stream and did not go through the center of the trapping position until about 0.2 sec after burning ceased. The 2-inch-long, 1/4-inch-diameter stainless tubing melted away and appreciable damage was done to the probe surface. No rocket exhaust gases or solids were trapped. The probe pressure transducer cable also melted.

The failure of this technique on the first sampling instigated several modifications of the probe and its instrumentation: A 1.25-inch-diameter tantalum rod was machined for the stainless steel fitting on the apex of the probe; the hydraulic drive system was modified to give a direct 100% maximum force drive rather than a linked (60%) drive; a maximum pressure of 150 psi was used to actuate the hydraulic piston; and a copper shield was placed above the probe to protect the probe pressure transducer cable.

Run 1. A 5x7 inch engine containing ANP-2699 propellant was fired and the probe (incorporating the above modifications) was passed through the exhaust. The probe was located so that, when in the axis of the rocket, the tip was 0.125 inch away from the exit plane of the nozzle. Figure 4 shows the probe in two positions of its motion through the exhaust (axially and perpendicular to the rocket), as well as the locus of the tip of the probe in its travel. The probe sweep was at the maximum rate, one sweep per second. The check valve inside the probe failed during this test; the Teflon float was distorted and coated with particles which did not permit the float to seat properly when the

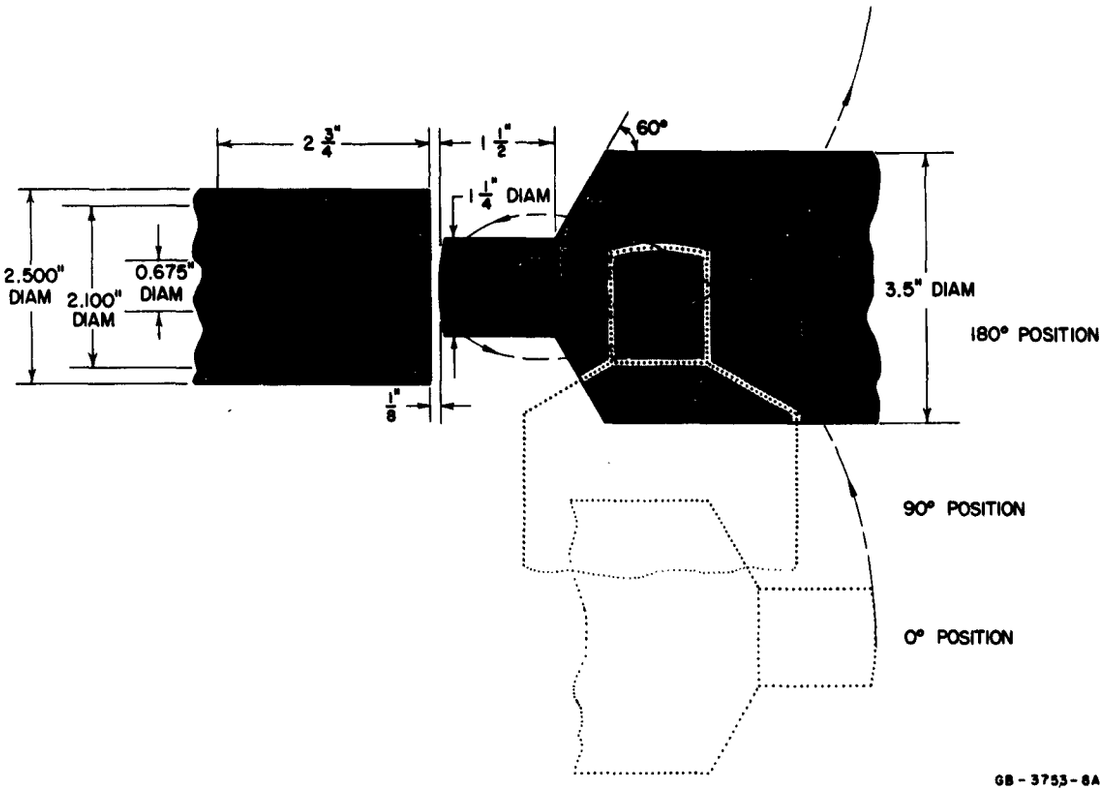

FIG. 4 ORIENTATION OF THE PROBE INITIALLY, AND PERPENDICULAR AXIAL TO THE NOZZLE

valve was closed, thereby allowing the trapped gases to escape and diffuse with the surrounding atmosphere. In addition, the steel spring in the check valve failed because a segment of it melted. The probe pressure transducer cable performed adequately. The "O"-ring closures at the rear of the probe did not hold a vacuum; in fact, liquid nitrogen coolant leaked visibly from the probe. The tantalum tip performed satisfactorily with only a minimum amount of eroding on the circular edge. The stainless steel front plate was eroded slightly and was covered with a thick coating of rocket exhaust solid product. The tip and probe after this firing are shown in Fig. 5. A very small amount of solid exhaust product was found inside the probe; however, inspection

of the product revealed that it was contaminated with iron from the check valve. Color motion pictures of the travel of the probe through the exhaust were taken; a high speed, rotating-prism shutter Fairchild motion picture camera was used at a rate of 100 frames/sec at f19.

FIG. 5 PROBE AFTER SUBJECTED TO ROCKET EXHAUST

Run 2. A mouse-trap check valve located about six inches from the hot tantalum probe tip within the sampling chamber was employed and was found to fail because particulate matter adhered to the sealing surfaces. A small quantity of solid product was obtained. The probe was first cooled with liquid nitrogen prior to sampling; however, as the silicon "O" ring closures did not maintain the vacuum in the probe, the probe was permitted to warm up to a temperature at which the "O" rings performed adequately.

Run 3. Because of difficulties encountered previously with liquid nitrogen cooling, as well as a required 90-minute period to attain that temperature, the probe was not cooled again in the remaining tests; it was felt that a temperature differential of 2223°K had little to offer over a 2000°K differential in view of the difficulties of maintaining a vacuum. No check valve was incorporated in this experimental design; the probe

was vacuum-sealed by means of a 0.020-inch-thick polyethylene diaphragm which was wrapped around the probe tip (which had been covered with Apiezon M grease) and fastened in place with rubber bands. As the probe moved through the exhaust, the membrane was destroyed immediately upon contact with the exhaust stream, and the pressure in the probe increased to a maximum of about 50 psi (in the trapping position 180°) and then dropped to one atmosphere. As quickly as possible (about 45 seconds after the firing), the tantalum tip was removed and replaced with a Teflon-lined cap to prevent further diffusion and expansion of the surrounding atmosphere into the probe. The gas in the probe then was expanded into a 1000-ml vessel for subsequent analysis. Color motion pictures of this and subsequent runs were taken through a didymium filter with a high speed, rotating-prism shutter Fairchild camera at a rate of about 600 frames/sec at f1.9. The exact position of the probe as it travels through the exhaust was determined by attaching a shaft from the yoke which in turn drove a potentiometer; the resistance across the potentiometer was related to the position of the probe. This measurement was easily instrumented and was recorded with the other ballistic parameters: thrust, chamber pressure, nozzle pressure, and probe chamber pressure. Figure 6 shows data typically obtained from these runs. For convenience three reference positions are located on the curve: perpendicular to the exhaust (i.e., when the probe has moved 90° and 270°) and axially in the exhaust (180°).

Run 4. The yield of the solid material was increased by reduction of the probe sweep time.

Run 5. Still more solid material was obtained when the bore in the probe tip was reamed at a 45° angle to a surface diameter of 0.31 inch. In this experiment near-black discrete hollow spheres, about 0.1 inch in diameter, were obtained. Some of these are shown in Fig. 7. Several of the spheres were dissected and all were found to be hollow. The inside surface of a sphere is shown in Fig. 8.

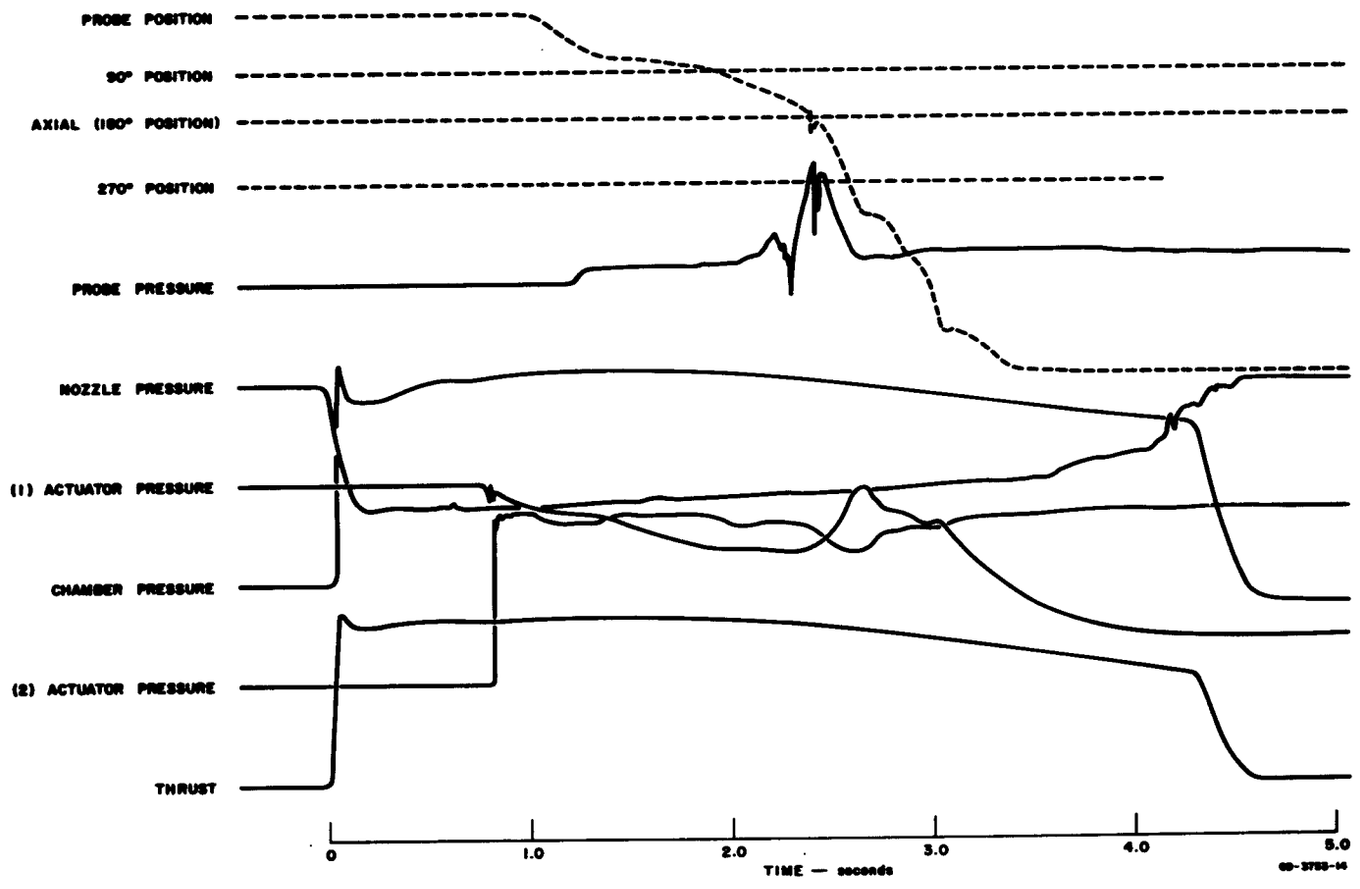

FIG. 6 RECORD OF BALLISTIC AND SAMPLING CHARACTERISTICS OF RUN NO. 7

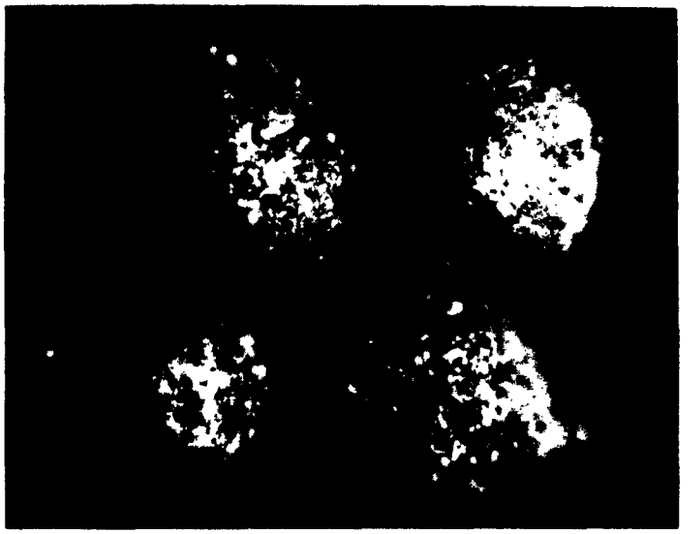

FIG. 7 TYPICAL PARTICLES OBTAINED FROM RUN NO. 5

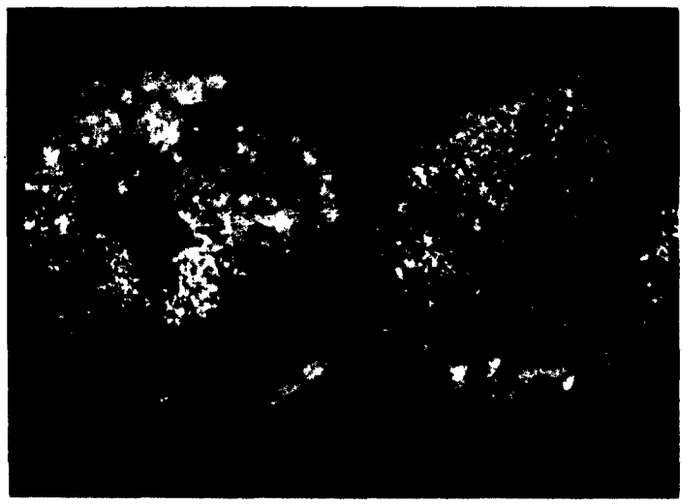

FIG. 8 INNER SURFACES OF DISSECTED PARTICLE FROM RUN NO. 5

Run 6. Improvement of the gas sampling was attempted by incorporating a double chamber design. The existing probe was partitioned with a removable circular plate which was sealed around its circumference with an "O" ring. The purpose of this plate was to keep the solid particles in the front chamber and permit the gases to expand through a check valve into the rear chamber. The impinging particles were deflected away from the check valve entrance with a cusp-type surface elevated above the partitioning plate. The double chamber in the probe is shown in Fig. 9. This double chamber technique failed in this instance because some of the solid particles did reach the check valve and did not permit the float to seat properly. The bore of the probe tip was enlarged to 0.31 inch and necessary modifications of the fittings on the probe were made so that a continuous 0.31-inch bore existed into the probe chamber. The pressure on each side of the hydraulic actuator piston was also measured throughout the travel of the probe. The typical behavior of these pressures is seen in Fig. 6. From these data it was determined that a pressure differential of 60 psi was necessary to drive the probe through the exhaust.

Run 7. The double chamber technique was not employed in this experiment. The 0.31-inch bore in the tantalum tip was reamed at a 45° angle to a surface diameter of 0.5 inch to increase the amount of solid matter trapped.

Run 8. A check valve similar to that used in Run 6 was utilized. A cylindrical jacket was placed around the cusp-type surface to restrict the flow of solid particles into the rear chamber. A new sealing method--a common rubber stopper on a film of Apiezon M grease--for maintenance of vacuum in the probe prior to sampling was found to be successful. The check valve did not hold because the particles did turn some six corners and adhere to the valve float which therefore did not seat properly.

Run 9. The operating parameters were identical to those in Run 8, but the check valve was modified slightly to restrict the flow of particles. Again, the gases were not trapped successfully.

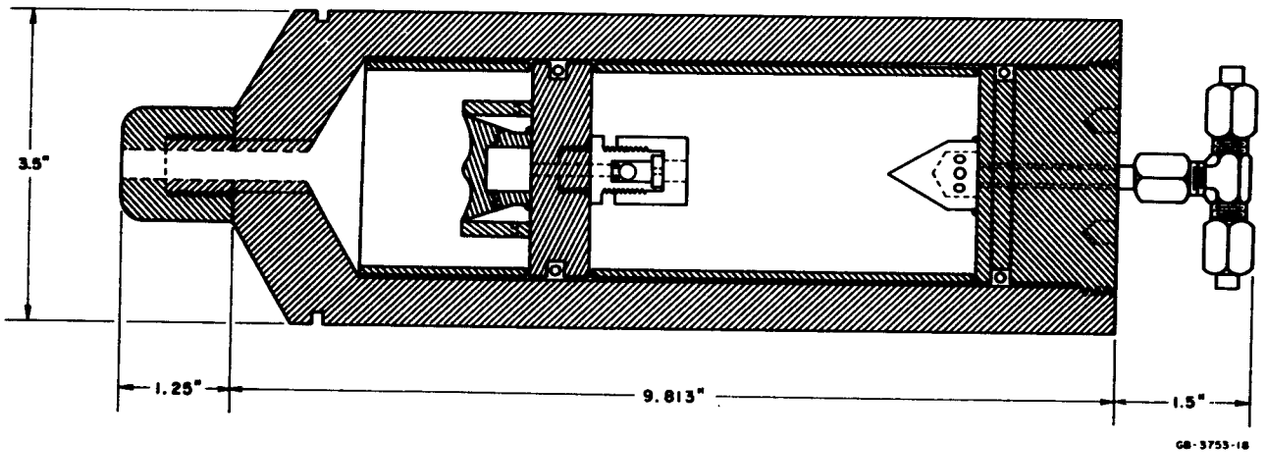

FIG. 9 MODIFIED PROBE SHOWING DOUBLE TRAPPING CHAMBER

Run 10. The sampling was performed at 1.56 inches from the exit plane. The check valve was not effective. The trapped solid matter was off-white in color.

Run 11. This was a reproducibility check on Run 10. The check valve was not effective.

Run 12. A poppet check valve (Fig. 10) was employed in this experiment and was found to be successful in maintaining the gases in the rear chamber at close to the maximum probe pressure. Otherwise, this experiment was performed using the operating parameters of Run 8. It was observed that a small amount of liquid was present in the gas chamber. This condensate was washed from the chamber walls with distilled water and transferred to a volumetric flask for subsequent analysis for acid and chloride content.

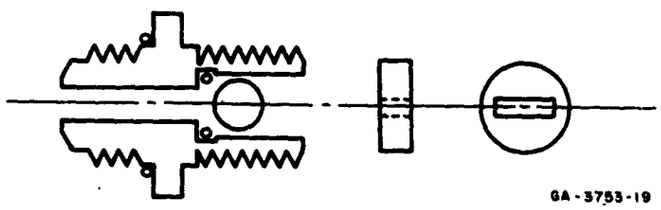

FIG. 10 POPPET CHECK VALVE

Run 13. This experiment was a repeat of Run 12. The condensate was also recovered in this experiment.

Run 14. The exhaust composition within the nozzle was sampled in this experiment. The tip of the probe was in the nozzle 0.25 inch ahead of the exit plane when the probe was axially in the exhaust (180° position). The records of ballistic and probe motion characteristics of this run are shown in Fig. 11. There is a small bump on the thrust-time curve which results from the probe being in the nozzle. The nozzle pressure curve ran off the scale in Run 14; to give completeness to this curve the nozzle pressure curve obtained for Run 17 is plotted in Fig. 11.

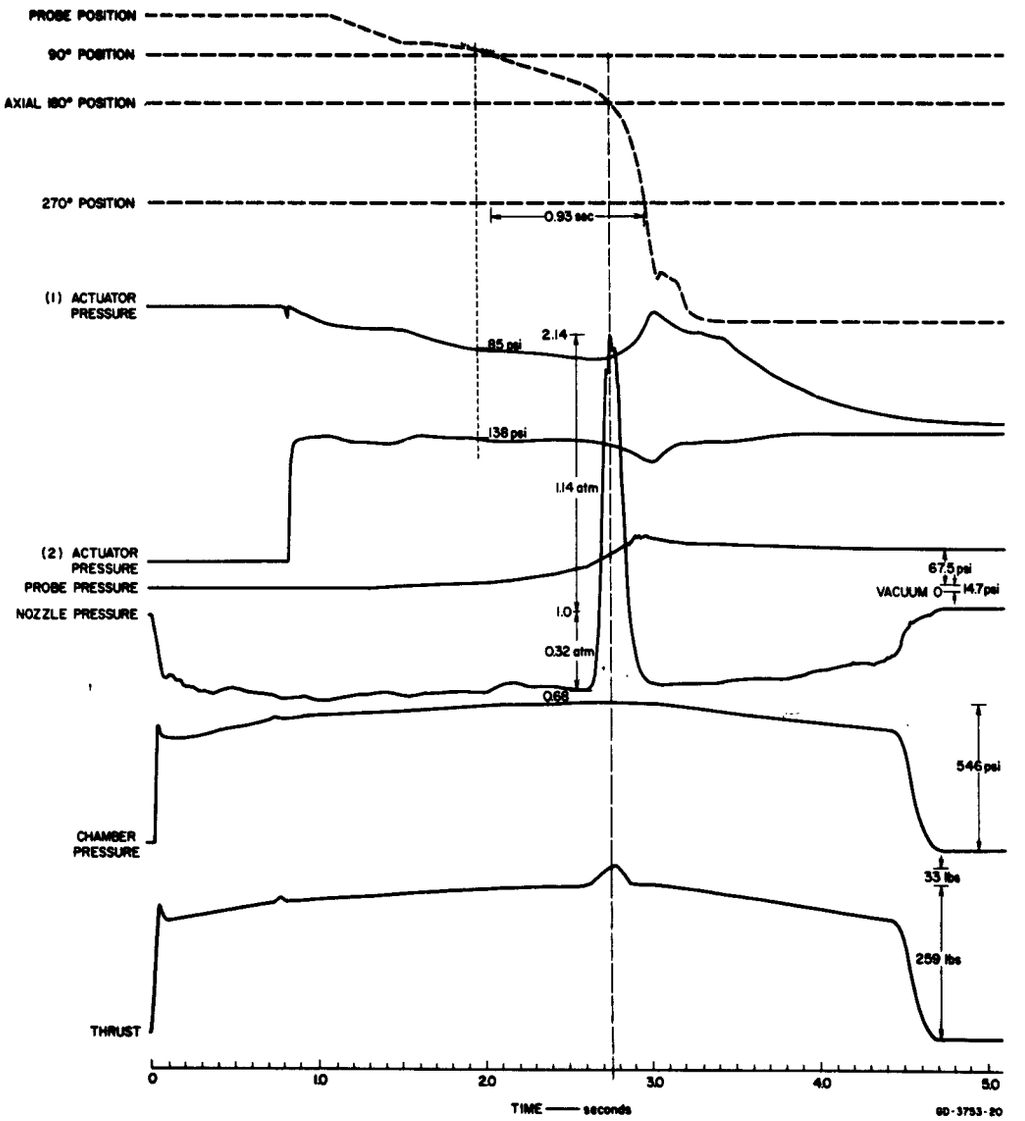

FIG. 11 BALLISTIC AND PROBE MOTION CHARACTERISTICS OF RUN 14. NOZZLE PRESSURE CURVE OF RUN 17

These curves otherwise are typical of those obtained when the gases are contained. The motion of the probe as it moves into the exhaust and nozzle is seen in the six selected frames from the motion pictures of the firing presented as Fig. 12: Fig. 12a--0.74 sec after ignition, probe facing the camera; Fig. 12b--2.02 sec, the probe tip entering the exhaust; Fig. 12c--2.26 sec, probe body entering the exhaust; Fig. 12d--2.67 sec, probe almost in 180° position; Fig. 12e--2.77 sec, probe at 180° (sampling) position; Fig. 12f--3.85 sec, hot tantalum tip facing camera at conclusion of probe's sweep.

Run 15. The effect of higher chamber pressure upon the exhaust composition was examined in this experiment. To this end, the following constricted nozzle configuration was utilized: throat diameter--0.615 inch, exit diameter-2.100 inches, and exit angle--15°. The trapping distance was 0.19 inch, the check valve was effective, and the condensate was recovered.

Run 16. The constricted nozzle (Run 15) was used in this run, with a trapping distance of 1.50 inches. The check valve was not effective. The trapped solid matter was off-white in color.

Run 17. The constricted nozzle was replaced with a nozzle with the original dimensions and the composition within the nozzle was sampled again. This run is essentially a repeat of Run 14. A photograph of a particle obtained from this run is seen in Fig. 13.

Run 18. The "O" rings in the check valve were replaced and the exhaust composition was sampled at 0.50 inch from the exit plane. The check valve proved effective and the condensate was recovered.

Run 19. This run was a reproducibility check of Run 14, in which the sample was obtained at 0.25 inch within the nozzle.

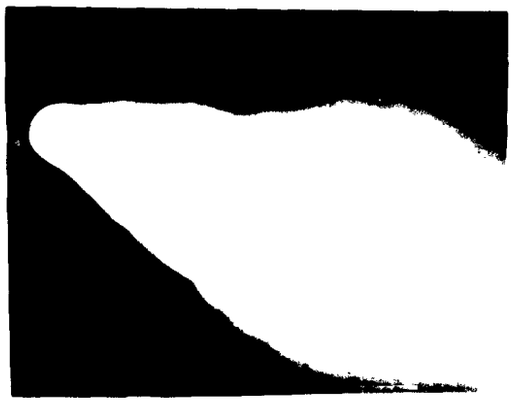

(a) 0.74 seconds

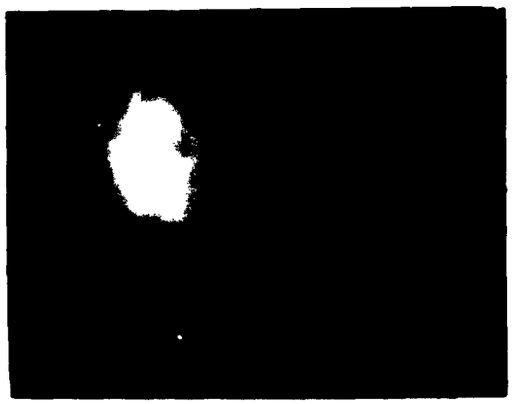

(b) 2.02 seconds

(c) 2.26 seconds

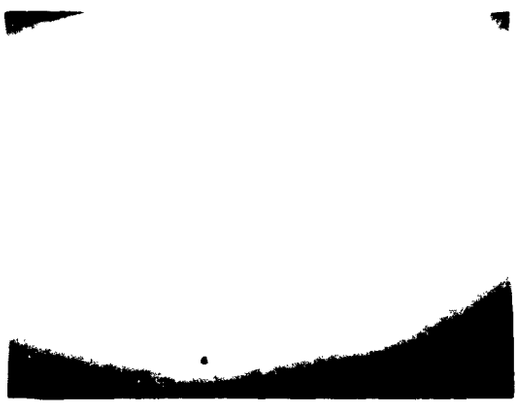

(d) 2.67 seconds

(e) 2.77 seconds

(f) 3.85 seconds

FIG. 12 POSITION OF PROBE IN EXHAUST STREAM AT VARIOUS INTERVALS AFTER IGNITION

FIG. 13 A PARTICLE OF SOLID MATTER OBTAINED FROM RUN 17

D. Exhaust Sampler for Use at Aerojet-General

Use of the findings of the previous 20 firings at the Calaveras Test Site permitted a sound design of a probe and hydraulic actuator for sampling 3KS-1000 motors at Aerojet-General. The new probe incorporated the important features developed earlier: (1) tantalum tip and 1/4-inch face shield, (2) double sampling chamber, and (3) poppet check valve. The new probe is shown in Figs. 14 and 15. A new hydraulic actuator and its stand were designed and fabricated to meet the requirements for its use at Aerojet-General.

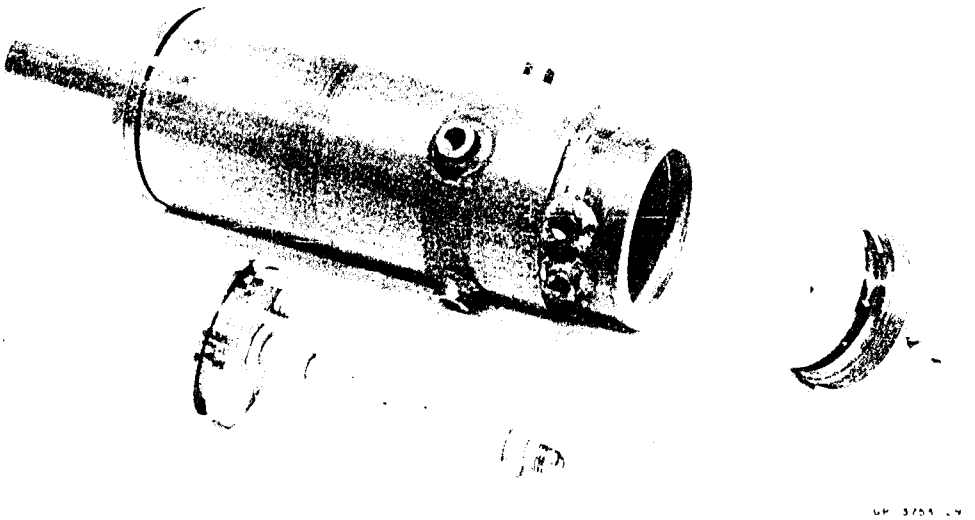

FIG. 14 DISASSEMBLED ROCKET EXHAUST SAMPLING PROBE

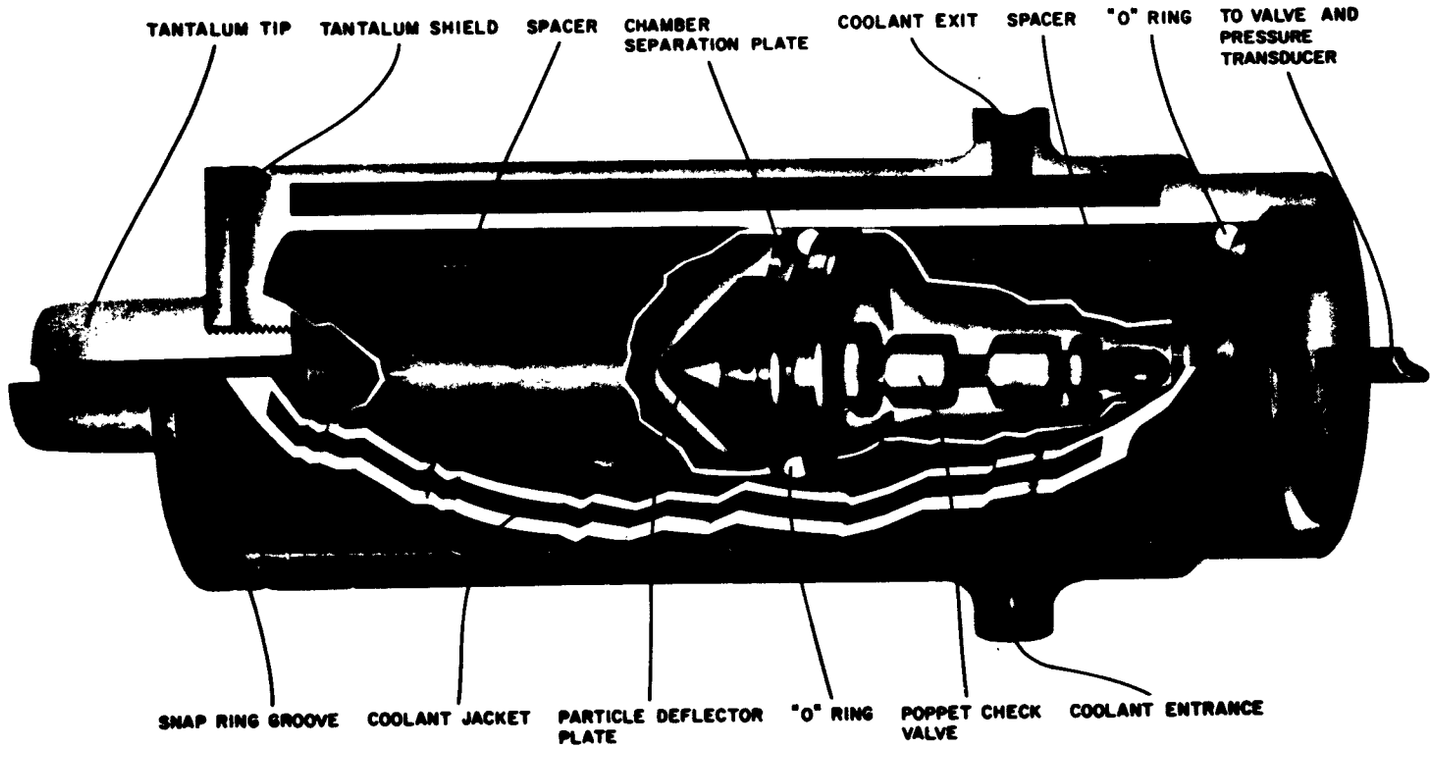

FIG. 15 CUT-AWAY DRAWING OF ASSEMBLED PROBE

This actuator incorporates a Hannifin Series A air power cylinder to drive the probe through the exhaust stream. Figure 16 is a photograph of the probe, actuator, and stand. The probe is in the 180° trapping position. A better view of the probe and actuator is seen in Fig. 17. Easily observed is the positioner (gear track and potentiometer). The bearings of the actuator are hidden from view by heat shields.

The probe (see Appendix L, Fig. L-1) was fabricated with a flat face so that a tantalum heat shield could readily be placed on its surface. The probe tip (Fig. L-2) was a 4-inch-long, 1-1/4-inch-diameter tantalum rod with an 0.31-inch axial hole, and one end of the probe tip was threaded to mate with the probe's front-face orifice. The particle-deflecting plate (Fig. L-3) was located about 5.3 inches from the tip of the probe. The configuration used maintained roughly the same distance from tip of the probe to the particle deflector plate as previously employed, but permitted a smaller mass to be present in the exhaust during the motion of the probe. Detailed drawings of the probe, hydraulic actuator, and their accessories are found in Appendix L.

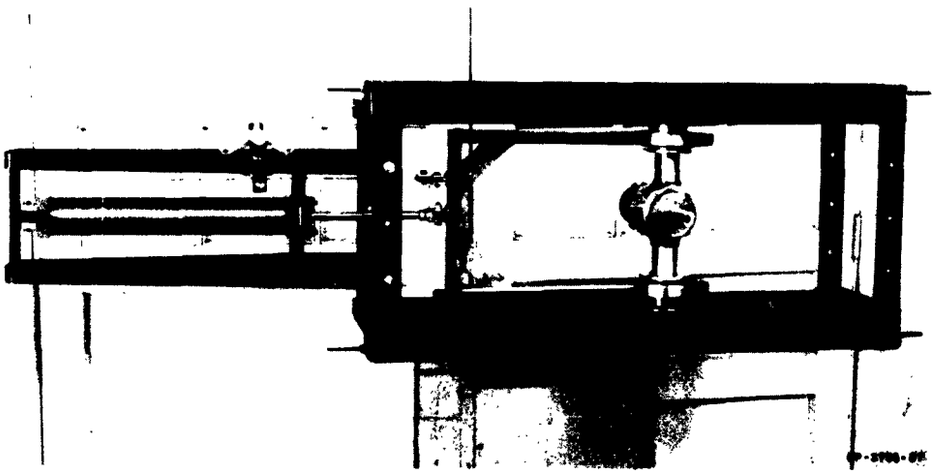

FIG. 16 PROBE, HYDRAULIC ACTUATOR, AND STAND

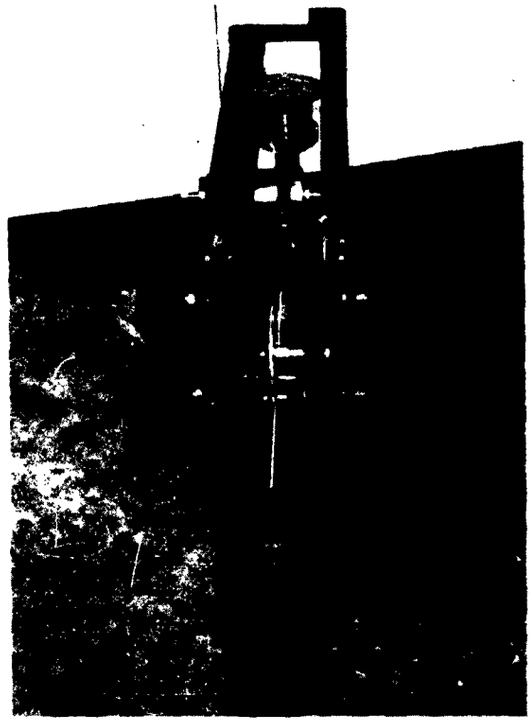

FIG. 17 SIDE VIEW OF PROBE AND HYDRAULIC ACTUATOR

E. Experiments at Aerojet-General

The completed probe, hydraulic actuator, and stand were transferred to Aerojet-General, Nimbus, California, and the exhausts of eleven rocket motors were sampled. Because the new sampler had been enlarged and a new actuator was employed, it was necessary to change the values of several operational parameters from those used in the Calaveras Test Site sampling. A summary of these parameters are listed in Table III.

Table III

OPERATIONAL PARAMETERS AND RESULTS OF FIRINGS
AT AEROJET-GENERAL CORPORATION

Run MM-DF-16S-BH	Lag in motion of probe (sec)	Sweep Time			Total Firing Time (sec)	Chamber Pressure at 180° position (psig)	Solid matter trapped (g)	Gases contained (atm)
		Total (sec)	90° to 270° (sec)	Time from ignition to 180° (sec)				
30	a	a	a	a	4.22	a	0.06	3.0
31	0.75	3.19	2.13	1.45	4.75	a	2.13	1.0
32	0.79	3.24	2.29	1.45	5.02	a	0.96	1.0
49	0.64	2.67	1.74	2.81	3.70	1109	6.34	1.0
50	0.59	1.46	0.93	1.63	3.80	918	4.60	0.5
51	0.71	1.49	0.97	1.77	3.82	960	6.43	c
52	0.61	1.49	0.97	1.70	3.69	958	5.63	1.0
53	0.62	1.49	0.98	1.67	3.68	962	5.37	0.3
54	0.72	1.54	1.02	1.82	3.19[b]	817	2.68	0.4
55	0.65	1.52	0.99	1.72	3.43	798	2.40	1.1
56	0.78	1.59	1.04	1.94	3.37	847	2.67	0.7

a/ No data obtained

b/ Nozzle insert failed during firing

c/ Air leak in line

The large capacity of the Hannifin Series A air power cylinder incorporated in the system caused a relatively long probe-sweep time, in the order of 3.5 sec. Because the duration of the high pressure portion of the motor firing was about 3.7 sec, and a lag in actuation of about 0.8 sec was anticipated, the probe was actuated about 1.5 seconds prior to ignition of the propellant.

Sampling was accomplished with the probe arranged so that at the 180° position the probe tip was just in the exhaust plane. The physical arrangement of the probe in the 180° position with respect to the nozzle at the Aerojet-General test stand is seen in Fig. 18. The entire apparatus--supports, hydraulic actuator, probe, rocket motor, and test stand--is shown in Fig. 19.

At the conclusion of runs MM-DF-16S-BH-30 to BH-32 the following modifications were incorporated to facilitate efficient sampling:

1. The length of the tantalum tip was reduced to 2 inches to permit a larger sample to be collected.
2. A new magnetic solenoid valve with 0.125-inch ports was installed on the hydraulic actuator at Aerojet-General to permit better control on the probe sweep cycle.
3. A stainless steel gasket was incorporated in the probe gas check valve, replacing the Teflon seating in order to permit proper closure of the valve.
4. Two stainless steel cylindrical spacers were fabricated for use in changing the volume of the two chambers of the probe, so that the distance from the nozzle exit plane to the particle-deflecting plate could be varied.

Some difficulty was encountered in removal of the chamber separation plate when the probe was dismantled for recovery of the solid sample. This difficulty arose from inadvertent tilting of the plate, scraping of the Teflon layer, and subsequent jamming of the plate in the probe. To prevent this difficulty in future experiments, a device for removal of the plate was fabricated and is shown in Fig. 20.

In spite of the success of the poppet check valve to maintain the exhaust gases in the tests at the Calaveras Test Site, this valve operated properly only once in the Aerojet-General tests.

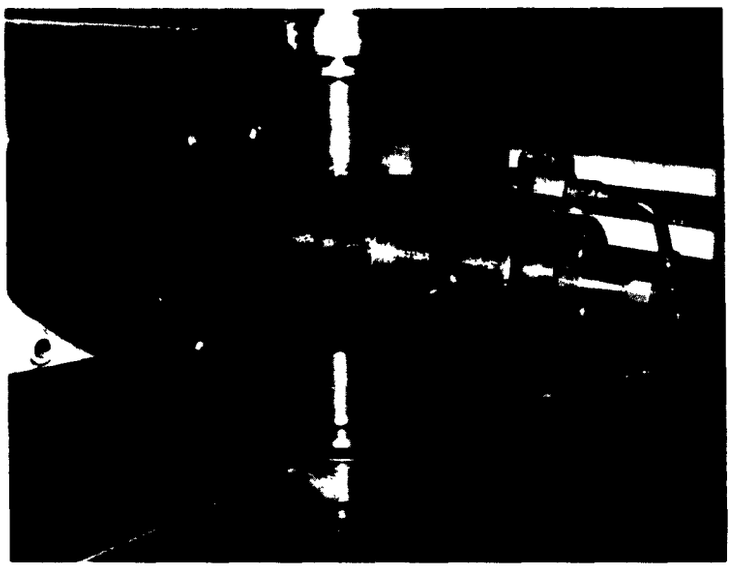

FIG. 18 PROBE AT 180° POSITION

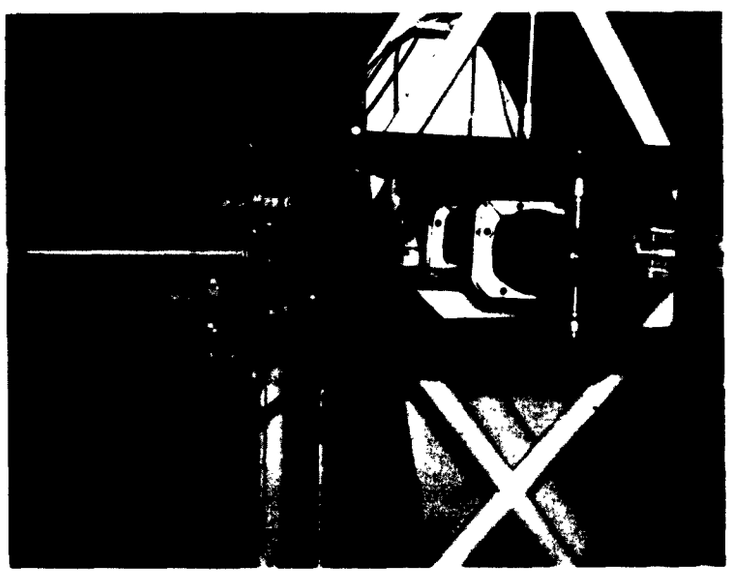

FIG. 19 PROBE AND HYDRAULIC ACTUATOR ATTACHED TO AEROJET TEST STAND

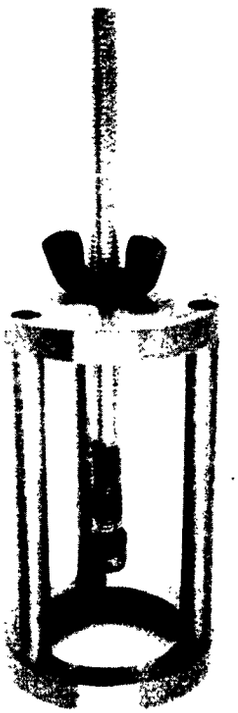

RP-3753-4

FIG. 20 DEVICE TO ASSIST IN REMOVAL OF CHAMBER SEPARATION PLATE FROM PROBE

V EXHAUST PRODUCT ANALYSIS

The results of the analysis of the exhaust products are categorized according to their physical state at ambient temperatures and site of sample origin.

A. Calaveras Test Site Firings

1. Solid Products

Results of the analysis of the composition of the solid material trapped at the Calaveras Test Site are listed in Table IV. Because of the small quantities obtained in Runs A, 1, 2, 3, and 4, analysis of these products was not justified. The repeatability of the results is not desired. These variations may have arisen from difficulties in obtaining a uniformly homogeneous sample. Sampling was performed by crushing the material manually with an agate pestle in an agate mortar, then mixing the particles thoroughly; the material was quite hard, and the average particle size was relatively large (about 150μ).

The crushed material was subject to analysis by X-ray diffraction. The results of all the sample analyses were quite similar and only minor intensity variations were observed when comparisons were made between samples. The diffraction pattern of the solid product obtained, from Run 14, typical of all, is presented in Fig. 21.

The principal lines in the patterns matched those of a alumina; the crystal spacings are listed in the figure. Most of the remaining lines matched those of rutile, TiO_2; however, one rutile line was missing. Chemical analysis did not confirm the presence of significant quantities of titanium; the presence of appreciable quantities in the rocket exhaust is quite surprising. Lines for metallic aluminum, carbon, ferric oxide, iron, aluminum carbide, and aluminum oxycarbide were not observed. However, iron and aluminum carbide have been observed by chemical analysis and visual inspection. These conflicting facts are not easily

Table IV

CHEMICAL ANALYSIS OF SOLID EXHAUST PRODUCTS*

Run	%Al		$\%Al_2O_3$		$\%H_2O$		%C		$\%Fe_2O_3$		$\%Ta_2O_5$[b]
	Value	Std. dev.	Value	Std. dev.	Value	Std. dev.	Value	Std. dev.	Value	Std. dev.	
5	a	a	80.1	1.8	0.86	0.12	0.16	0.01	0.61	0.11	a
6	1.62	0.17	71.3	1.6	0.91	0.10	0.12	0.02	1.13	0.20	a
7	2.34	0.09	83.4	2.1	1.37	0.11	0.25	0.01	1.28	0.04	10.6
8	1.42	0.48	74.3	3.4	0.67	0.20	0.10	0.01	2.73	0.15	17.3
9	1.48	b	82.0	2.3	0.79	b	0.12	b	0.41	0.09	5.9
10	-0.02	b	84.4	6.2	0.30	b	0.05	b	1.23	0.12	4.0
11	0.15	0.01	82.0	0.2	0.31	0.15	0.05	0.01	0.97	0.13	3.1
12	1.61	0.25	75.7	4.1	1.21	0.16	0.06	0.04	0.75	0.10	4.4
13	1.94	0.20	74.5	2.6	1.00	0.16	0.19	0.03	2.49	0.49	19.4
14[c]	2.34	0.18	75.3	0.2	1.01	0.16	0.14	0.03	1.10	0.33	21.3
15	0.66	0.26	76.4	0.5	0.97	0.13	0.34	0.03	0.70	0.03	23.6
16[d]	-0.01	0.03	84.5	0.2	0.63	0.14	0.25	0.03	0.43	0.04	a
17	2.49	0.33	72.8	3.8	1.06	0.28	0.08	0.04	0.55	0.09	a
18	0.92	0.21	75.9	3.4	1.15	0.10	0.18	0.03	1.88	0.20	a
19	2.67	0.24	71.3	0.4	1.23	0.28	0.23	0.03	1.01	0.26	a
Pooled Std. dev.		0.23		2.8		0.17		0.03		0.20	

a Not determined
b No replication obtained
c Sample contained 0.06% titanium
d Sample contained 0.01% titanium

* Motor firings at Calaveras Test Site

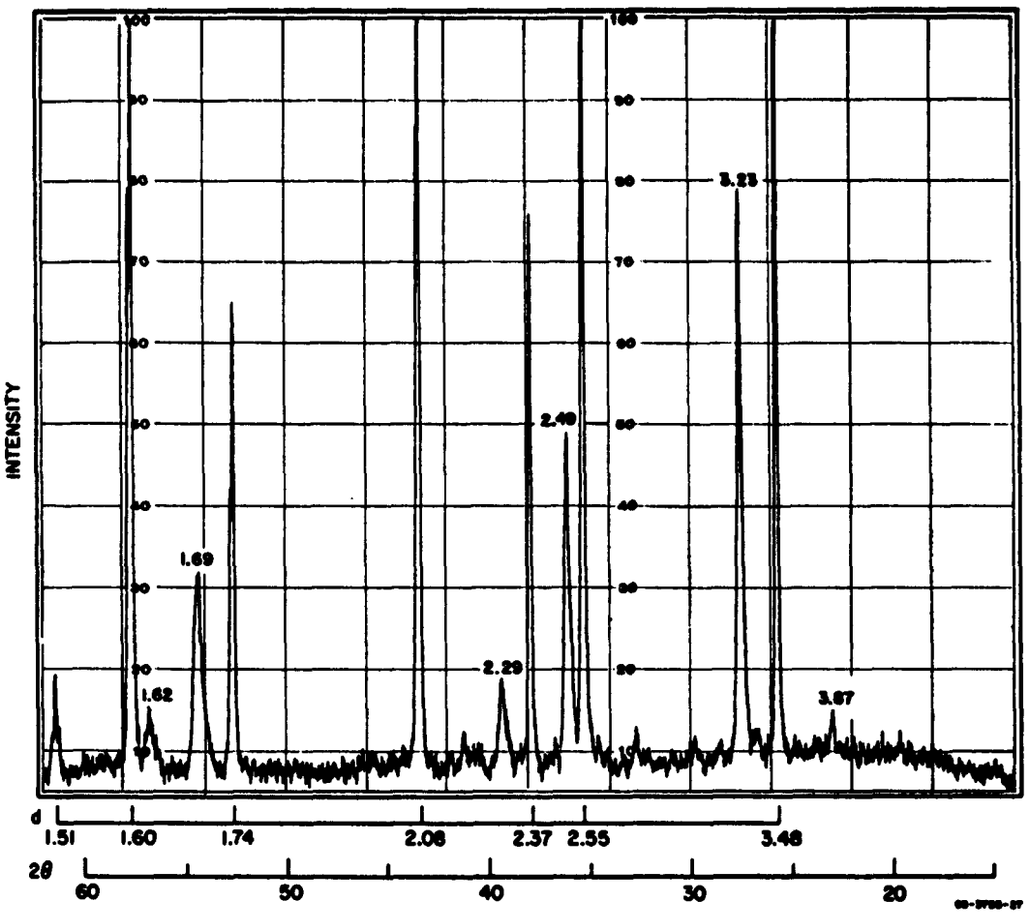

FIG. 21 TYPICAL X-RAY DIFFRACTION PATTERN OF SOLID PRODUCT (Run No. 14)

resolved. The concentration of iron and aluminum carbide is low, and X-ray diffraction may not have sufficient sensitivity to show these structures. The unidentified lines which resemble those for rutile most likely stem from the presence of tantalic oxide, a material whose X-ray spectra have not yet been investigated in any detail.

The presence of aluminum carbide in the solid product has been ascertained from its yellow color and its reaction with water. It most likely forms from reaction of alumina with the nozzle[16] (Eq. 7)

$$2Al_2O_3 + 9C \longrightarrow Al_4C_3 + 6CO \qquad (7)$$

The results presented in Table IV do not consider the presence of Al_4C_3. Its presence would be accompanied by an increase in weight of the combustion boat (Eq. 8)

$$Al_4C_3 + 6O_2 \longrightarrow 2Al_2O_3 + 3CO_2 \qquad (8)$$

that is,

$$\text{weight increase} \approx (0.417)\,(\text{wt carbide}) \qquad (9)$$

also,

$$\text{carbon dioxide evolved} = (0.917)\,(\text{wt carbide}) \qquad (10)$$

If it is now assumed that all the carbon dioxide found in the combustion method came from the carbide and not from elemental carbon, the equation for calculation of the percent free-aluminum changes

from $$\%Al = \frac{100\delta}{w} + \%H_2O + \%C \qquad (11)$$

to $$\%Al = \frac{100\delta}{w} + \%H_2O - 1.67(\%C) \qquad (12)$$

where δ is the weight increase of the boat and w is the weight of sample. It would follow then that the free-aluminum results listed in Table IV might be high by as much as 2.67(%C). If this correction is applied to the data in Table IV we find that the results are lowered somewhat, and in two instances (Runs 15 and 16) the resultant value is significantly below zero (an impossible result). Obviously the answer lies somewhere between these extremes.

The nature of the trapped iron species and its role in the combustion analysis have been considered in detail. If the metal is oxidized to Fe_2O_3 by the exhaust stream, it would have no effect on the results. However, if it ablates as the free metal it would cause the weight to increase. Because there is no correlation between aluminum concentration and the iron oxide level (Table IV), it can be inferred that the weight increase of the boat is not due to oxidation of iron.

To calculate the percent unburned aluminum it is necessary to substitute the data for aluminum and aluminum oxide in the following equation:

$$\text{Percent unburned} = \frac{100(\%Al)}{(\%Al + 0.530(\%Al_2O_3)} \qquad (13)$$

2. Gaseous Products

The results of the analyses of the gaseous exhaust products are listed in Table V on a hydrogen chloride-, water-, and air-free basis. This basis was chosen because water condenses in the probe chamber (the maximum pressure of water in the gas phase is 1.75 cm Hg at 20°C) and sufficient time is not allowed to attain equilibrium in the transfer to the gas-collecting bulb. To complicate matters further, hydrogen chloride is very soluble in water; hence its concentration is reduced from the expected value. Small quantities of air (evaluated from the oxygen content arising from leakage or from being trapped prior to entry of the probe into the exhaust stream) have no bearing on the exhaust composition.

The agreement between the different methods is poor in some instances; however, on the whole it is good. All the analytical methods used assume the validity of the perfect gas law. However, this assumption is strictly valid only for analyses by mass spectrometry. Consequently, if a choice must be made, it is recommended that the results of the mass spectrometric analyses be used.

The results from Tables I and V show that the CO_2 /CO ratio increases with distance beyond the exit plane.

B. Aerojet-General Test Site Firings

1. Solid Products

The results of the determinations of aluminum, aluminum oxide, carbon, water, ferric oxide, and tantalum oxide in the solid exhaust products obtained from the firings at Aerojet are listed in Table VI. The total aluminum, iron, and tantalum determinations were not obtained for Run MMDF-16S-BH-30 because the amount of sample trapped (60 mg) was insufficient for these analyses.

Table V

COMPARISON OF ANALYSES OF GASEOUS EXHAUST PRODUCTS[a] *

Run	Method	Mole % N_2		Mole % CO		Mole % CO_2		Mole % H_2		CO_2 / CO
		Value	Std. dev.	Value	Std. dev.	Value	Std. dev.	Value	Std. dev.	
12	MS	28.48		26.62		3.68		41.22		0.138
	GSPC	27.44	1.51	25.64	0.02	3.55	0.42	43.37	1.29	0.139
	IR			24.50	0.37	3.66	1.30			0.149
13	MS	22.00		28.09		3.04		46.87		0.108
	GSPC	22.02	0.25	28.14	0.50	2.98	0.31	46.87	2.45	0.106
	IR			26.58	1.75	3.11	0.28			0.117
14	MS	16.28		31.48		1.55		50.69		0.049
	GSPC	15.33	1.42	29.65	0.44	1.39	0.05	53.65	2.30	0.047
	IR			28.07	1.24	1.51	0.17			0.054
15	MS	19.64		28.85		2.88		48.62		0.100
	GSPC	19.74	0.25	29.00	0.15	2.22	0.01	49.04	0.33	0.077
	IR			26.32	0.97	2.49	0.06			0.095
18	MS	21.68		29.62		2.51		46.19		0.085
	GSPC	21.42	0.12	29.25	0.49	2.40	0.23	46.93	0.55	0.082
	IR			27.14	0.48	2.46	0.05			0.091
19	MS	19.26		29.17		2.08		49.49		0.071
	GSPC	18.54	0.31	28.10	0.07	2.32	0.46	51.05	2.19	0.082
	IR			26.67	1.87	1.84	0.04			0.069
8	GSPC	30.26	0.55	30.57	0.07	4.47	0.09	34.69	0.54	0.146
	IR			29.44	1.25	4.06	0.21			0.138
9	GSPC	40.24	0.34	23.29	0.77	4.36	0.19	32.11	1.22	0.192
	IR			23.32	1.32	4.84	0.19			0.207
11	GSPC	39.65	1.11	23.71	0.00	6.02	0.02	30.62	0.80	0.254
	IR			21.43	1.29	6.18	0.28			0.288
16	GSPC	28.11	0.69	28.27	1.21	4.16	0.09	39.46	0.77	0.147
	IR			28.34	1.18	4.82	0.22			0.170
17	GSPC	22.87	0.30	28.15	0.27	2.84	0.05	46.15	1.04	0.101
	IR			26.96	0.95	3.03	0.01			0.112

a/ Calculated on a HCl-, H_2O-, and air-free basis. * Motor firings at Calaveras Test Site

Table VI

CHEMICAL ANALYSIS OF SOLID EXHAUST PRODUCTS FROM MOTOR FIRINGS AT AEROJET-GENERAL CORPORATION

Runs MMDF	Component, Weight Percent											
	% Al		% Al_2O_3		% C		% H_2O		% Fe_2O_3		% Ta_2O_5	
16S-BH	Avg.	Std. dev.	Avg.	Std. dev.	Avg.	Std. dev.	Avg.	Std. dev.	Avg.	Std. dev.	Avg.	Std. dev.
30	-0.05	a	b	b	0.09	a	0.36	b	b	b	b	b
31	0.63	0.06	72.30	1.80	0.28	0.03	0.77	0.06	3.44	0.09	19.00	a
32	0.25	0.06	78.10	1.30	0.20	0.02	0.82	0.19	7.32	a	14.80	a
49	0.55	0.07	84.88	0.62	0.44	0.08	0.36	0.08	0.28	0.08	14.60	b
50	0.69	0.04	81.29	0.91	0.27	0.01	0.45	0.08	0.15	0.07	9.87	.81
51	0.73	0.20	84.57	0.50	0.49	0.10	0.50	0.02	0.22	0.04	5.63	1.22
52	0.88	0.19	88.69	0.61	0.56	0.09	0.50	0.18	0.27	0.01	9.28	0.80
53	0.63	0.14	86.67	2.28	0.46	0.08	0.55	0.09	0.17	0.03	4.73	0.41
54	0.07	0.07	84.42	3.76	0.02	0.02	0.41	0.10	0.15	0.02	3.70	0.03
55	0.04	a	85.28	1.43	0.07	a	0.27	a	0.18	0.02	7.77	0.23
56	0.04	0.08	82.49	1.35	0.06	0.04	0.38	0.10	0.35	0.01	3.49	0.39
Pooled Std. dev.		0.12		1.83		0.06		0.11		0.05		0.67

a/ No replicate determination

b/ Not determined

The ammonium-perchlorate and aluminum compositions of the propellants used in these firings together with significant observations and motor configurations utilized are listed in Table VII. The average metallic aluminum content in the exhaust of propellant with NH_4ClO_4/Al = 3.7 was 0.70% in the solid exhaust product, or approximately 1.5% unburned aluminum. On the other hand, the average metallic aluminum content in the exhaust of propellant with NH_4ClO_4/Al = 7.5 and 26.7 was respectively 0.05% and -0.05% or approximately 0.11% unburned aluminum. This latter value is nearly equivalent to the error in the method. Concurrent with these differences in metallic aluminum content, the average carbon content in the sample with 1.5% unburned aluminum was 0.44%, while with 0.10% unburned aluminum 0.05% carbon was present.

2. Gaseous Products

The results of the analyses of the gaseous exhaust products of the June 6-7 firings have been completed and are listed in Table VIII on a hydrogen chloride-, water-, and air-free basis. The small amount of trapped gases is such that the accuracy of the infrared method and of the carbon dioxide determination by gas-solid partition chromatography may have suffered. For this reason the values from the analysis by mass spectroscopy (a technique which does not require a large amount of gas and in which the assumption of the validity of ideal gas law is most correct), are the preferred ones.

Table VII

PROPELLANT COMPOSITION AND SIGNIFICANT OBSERVATIONS OF SOLID EXHAUST PRODUCTS OBTAINED FROM AEROJET-GENERAL MOTOR FIRINGS

Run MMDF 16S-BH	$\%NH_4ClO_4$	% Al	Comment
30	80	3	Solid product - white
31	63	17	Black product
32	63	17	Standard motor half-filled to give longer residence time
49	63	17	Standard motor, black product
50	63	17	Standard motor, black product
51	63	17	Standard motor, black product
52	63	17	Standard motor, black product
53	63	17	Standard motor, black product
54	75	10	Standard motor, near white prod.
55	75	10	Standard motor, near white prod.
56	75	10	Standard motor, near white prod.

Table VIII
COMPARISON OF ANALYSIS OF GASEOUS EXHAUST PRODUCTS OF MOTOR FIRINGS AT AEROJET-GENERAL CORPORATION

Run[a] MMDF-16S-BH	Method	Component								
		Mole %N_2		Mole %CO		Mole %CO_2		Mole %H_2		
		Avg.	Std. Dev.	Avg.	Std. Dev.	Avg.	Std. Dev.	Avg.	Std. Dev.	CO_2/CO
30	GSPC IR	18.37	0.28	37.32 33.78	0.67 1.50	12.22 12.39	0.04 0.70	32.10	2.36	0.327 0.367
31	GSPC IR	19.19	0.00	30.72 28.06	0.11 2.26	1.22 1.28	0.04 0.11	48.87	0.80	0.040 0.046
32	GSPC IR	65.53	0.62	16.45 15.30	0.36 0.45	6.63 6.60	0.08 0.13	11.39	1.41	0.403 0.431
49	MS GSPC IR	35.0 31.60	0.00	23.5 25.06 24.00	0.46 0.02	2.3 2.16 2.38	0.08 0.12	39.2 41.18	0.61	0.098 0.086 0.099
50	MS GSPC IR	34.5 33.94	0.28	24.5 25.46 26.00	0.39 0.09	3.0 2.85 2.03	0.64 0.12	38.0 37.76	0.93	0.122 0.112 0.078
52	MS GSPC IR	61.6 59.15	0.21	14.0 15.00 12.35	0.71 0.16	3.3 3.21 4.30	0.87 0.05	21.1 22.15	0.86	0.236 0.214 0.348
53	GSPC IR	41.53	1.21	22.16 24.41	0.27 0.25	2.94 2.95	0.33 0.03	35.31	2.07	0.133 0.121
54	GSPC IR	60.98	1.82	14.05 17.09	0.81 1.66	6.92 9.40	0.08 1.33	18.05	0.87	0.493 0.549
55	MS GSPC IR	55.8 54.03	0.56	18.0 19.09 15.15	0.20 0.18	6.0 6.50 5.77	0.09 0.26	20.2 20.38	0.14	0.333 0.341 0.381
56	GSPC IR	45.42	0.34	21.83 18.42	1.80 0.16	4.36 4.22	0.22 0.05	28.39	0.21	0.200 0.229

a/ No gaseous sample was obtained from Run MMDF-16S-BH-51

VI INTERPRETATION OF RESULTS

It is unequivocally clear from the results of the analysis of the solid exhaust product that:

1. Complete combustion of the aluminum does not take place before the gases pass the exit plane of the nozzle.
2. Combustion continues in the exhaust stream and at a point a few inches from the exit plane it is essentially complete.
3. Increased chamber pressure decreases the unburned aluminum concentration.
4. The degree of combustion is enhanced as the ammonium perchlorate-to-aluminum ratio is increased.
5. Increased residence time in the combustion chamber increases the degree of combustion.

The aluminum concentration in the exhaust as a function of the distance from the nozzle exit plane is shown in Fig. 22. Although the spread in the data shows that relatively poor repeatability is obtained in sampling, the increased metallic aluminum content as the exit plane, and then the throat of the nozzle, is approached is undeniably real. By similar token, the few data obtained show that an increase in chamber pressure leads to more complete combustion.

The effect of ammonium perchlorate to aluminum ratio is striking: for runs MMDF-16S-BH-49 through BH-53, (NH_4ClO_4/Al = 3.7) a black product which contained local areas of yellow aluminum carbide was obtained; and for runs MMDF-16S-BH-54 through BH-56 (NH_4ClO_4/ %Al = 7.5), an off-white material was obtained. Visual comparisons of these two products can be made from Figs. 23 and 24 which show the solid product trapped from runs MMDF-16S-BH-53 and 54 respectively. This night and day visual contrast is the same as that found as a function of distance from the exit plane for a highly aluminized propellant. The effect of increased residence time is seen from the results of runs

MMDF-16S-BH-31 and 32. For these runs, one motor was only half-full, thus increasing the distance a particle of aluminum must travel before it escapes through the nozzle; this increased residence time decreased the metallic aluminum concentration in the exhaust about 60%.

Interpretation of the composition of the gaseous product is not as rewarding as that for the solid products. Because the probe causes a shock wave of its own, it was expected that the observed gaseous composition would be different from the theoretical; however, it was hoped that a useful correlation could be obtained and that the observed composition would be reproducible, although perhaps not truly representative of the exhaust composition. Considerable effort was expended to contain the gases to yield a good sample; however, most of the experiments were plagued with leaks in the check valve. The poppet-type valve appeared to be the solution to this problem; however, of the eleven firings at Aerojet-General, the check valve functioned properly only once. Of the 7 pieces of data for "good" samples, no satisfactory correlation between theoretical and observed gaseous composition was established.

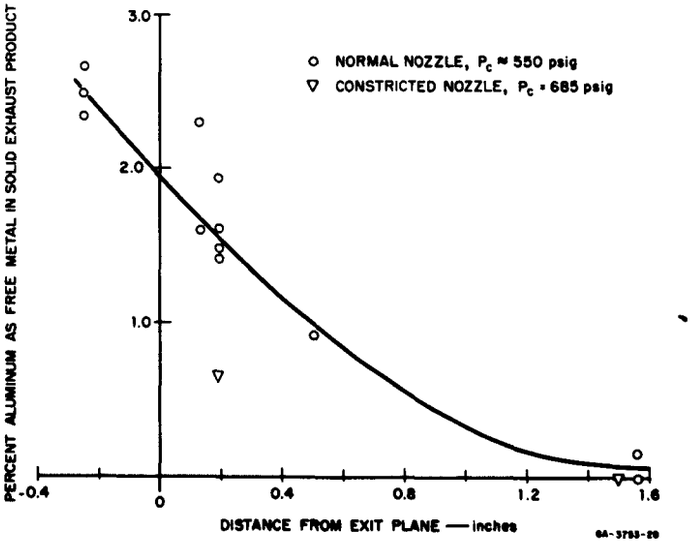

FIG. 22 CONCENTRATION OF METALLIC ALUMINUM IN SOLID EXHAUST PRODUCT AS A FUNCTION OF TRAPPING DISTANCE FROM NOZZLE

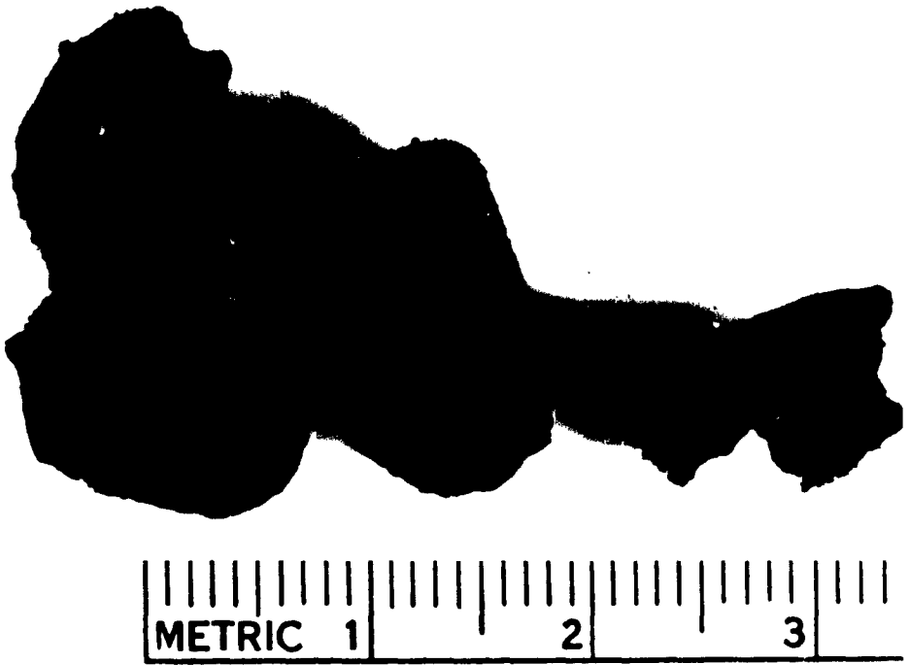

FIG. 23 TYPICAL EXHAUST PRODUCT AGGLOMERATES OBTAINED FROM SAMPLING AT NOZZLE EXIT PLANE OF PROPELLANT CONTAINING 17% ALUMINUM AND 63% AMMONIUM PERCHLORATE

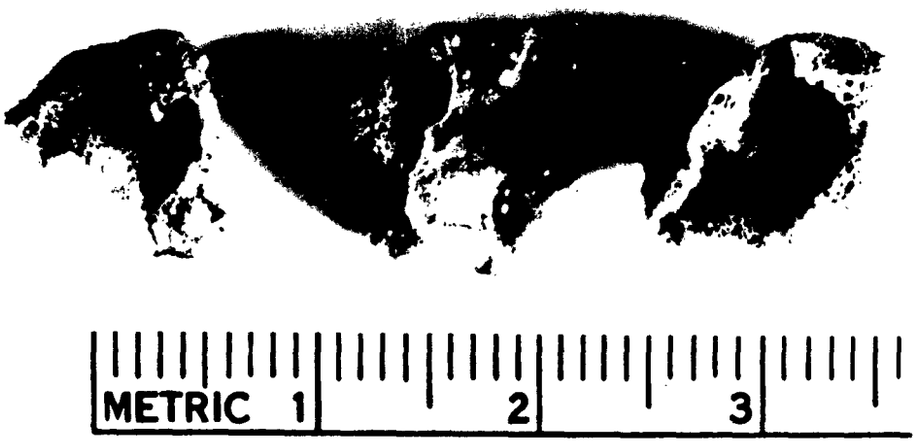

FIG. 24 TYPICAL EXHAUST PRODUCT AGGLOMERATES OBTAINED FROM SAMPLING AT NOZZLE EXIT PLANE OF PROPELLANT CONTAINING 16% ALUMINUM AND 75% AMMONIUM PERCHLORATE

ACKNOWLEDGMENTS

The author wishes to acknowledge the contributions, to the experimental work, of Mrs. J. Butler, Dr. D. A. Gordon, Miss E. A. Lawler, Mrs. A. P. Longwell, Mr. C. M. McCullough, and Mrs. J. S. Whittick to the experimental work, and to Dr. R. F. Muraca for many thought-provoking discussions.

REFERENCES

1. "Minuteman Stage III, Weapon System 133A." Hercules Powder Company Semi-annual Progress Report No. MCS-36 July-Dec. 1959, Contract AF 04(647)-243, CONFIDENTIAL
2. "Polaris Propellant Development", Aerojet-General Corporation Report No. 3606-01 QP-2, March-April (1960), Sacramento, 7 June 1960, CONFIDENTIAL
3. Brewer, L., and A. W. Searcy, J. Am. Chem. Soc. 73, 5308(1951)
4. Porter, R. F., P. Schissel, and M. G. Inghram, J. Chem. Phys., 23, 339 (1955).
5. [illegible]art, J., G. DeMaria, R. P. Burns, and M. G. Inghram, J. Chem. Phys., 32, 1366 (1960)
6. Hoch, M., and H. L. Johnston, "Formation and Crystal Structure of the Solid Aluminum Sub oxide: Al_2O and AlO". Ohio State University Research Foundation Technical Report No. 10, Project RF-280 Navy Contract N6ori-17, T.O. IV, August 1953.
7. Chupka, W. A., J. Berkowits, C. F. Giese, and M. G. Inghram, J. Phys. Chem., 62, 611 (1958)
8. Handbook of JANAF Panel on Analytical Chemistry of Solid Propellants, SPIA, Method JANAF 714.0-4(c). July 1959
9. "Research on Advanced Solid Propellants", Esso Research and Engineering Company Progress Report for Period December 11, 1959 through March 10, 1960, Contract No. DA-30-069-ORD-2487, p. 113, CONFIDENTIAL
10. Wannainen, F., and A. Ringbom, Anal. Chem. Acta. 12, 308(1955)
11. Meites, L., "Polarographic Techniques", Interscience Publishers, Inc., New York, 1955
12. Sandell, E. B., "Colorimetric Determination of Traces of Metals", Interscience Publishers, Inc., New York, 1959
13. Palilla, F. C., N. Adler, and C. F. Hiskey, Anal. Chem. 25, 926 (1953)
14. Pilinenko, A. T., and V. A. Obolontsik, Voprosy Poroshkovoi Met. Prochnosti Materialov, Akad. Nauk Ukr. S. S. R., 132 (1960)
15. Gordon, L. J., and J. M. Hoagland, "Effect of Nonideal Combustion and Gas Flow on Propellant Performance, "Bulletin of the 15th JANAF Solid Propellant Meeting, held at Washington, D. C., Vol. VI, p. 89, June 1959. CONFIDENTIAL
16. Foster, L. M., G. Long, and M. S. Hunter, J. Am. Cer. Am. Soc., 39,1 (1956).

APPENDIX A

INFRARED ANALYSIS OF GASEOUS EXHAUST PRODUCTS

INFRARED ANALYSIS OF GASEOUS EXHAUST PRODUCTS

The infrared spectrum of the gaseous exhaust products is obtained at a pressure of 15 to 20 cm Hg. The cell is pressurized with nitrogen to 40.0 cm Hg and again the spectrum is obtained. This operation is repeated at a total pressure of 70.0 cm. In this manner, confidence in the analytical determination is gained through replication. Also, replication at two different wave numbers is made. For hydrogen chloride, the concentration is determined at about 2940 and 2820 cm^{-1}; for carbon dioxide at about 2355 and 2340 cm^{-1}; for carbon monoxide at about 2170 and 2120 cm^{-1}. The concentration of the component is determined by relating the absorbance (measured via the base-line technique), at a particular wave length, to the pressure of the component with the aid of a calibration curve. Two calibration curves for each component are presented in Figs. A-1, A-2, and A-3 (hydrogen chloride, carbon dioxide, carbon monoxide, respectively). A typical spectrum of the exhaust gases obtained with the Perkin-Elmer model 221 Infrared Spectrometer used in this work is shown in Fig. A-4.

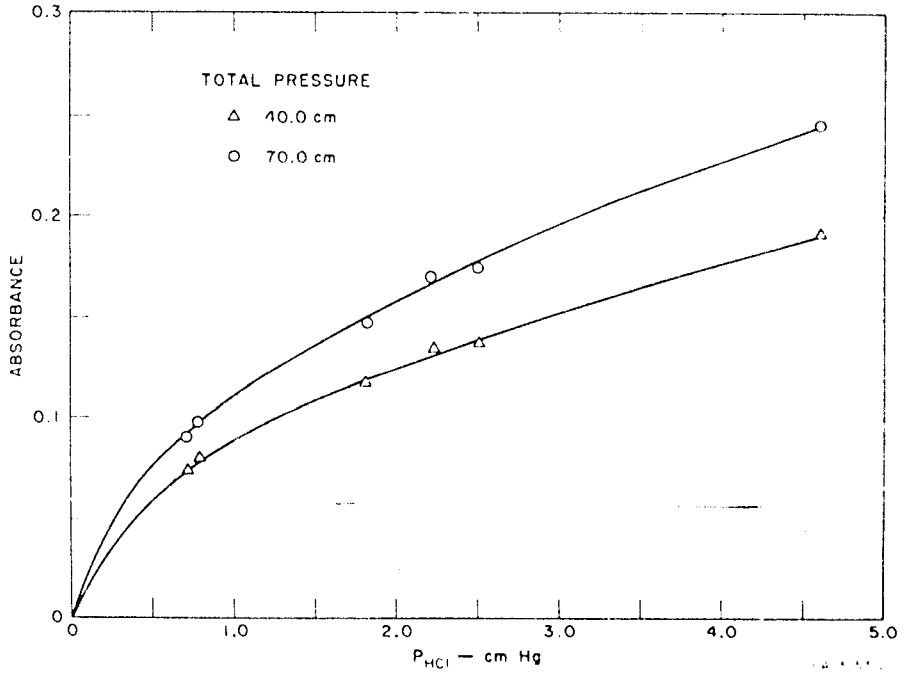

FIG. A-1 CALIBRATION CURVE FOR 2820 cm^{-1} PEAK OF HYDROGEN CHLORIDE

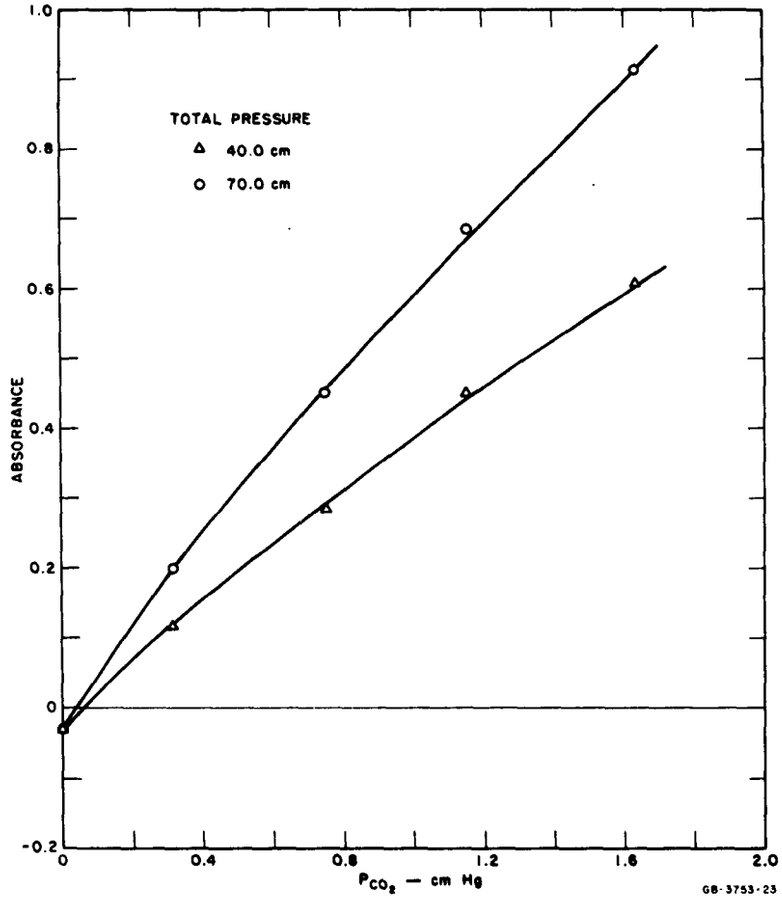

FIG. A-2 CALIBRATION CURVE FOR 2340 cm^{-1} PEAK OF CARBON DIOXIDE

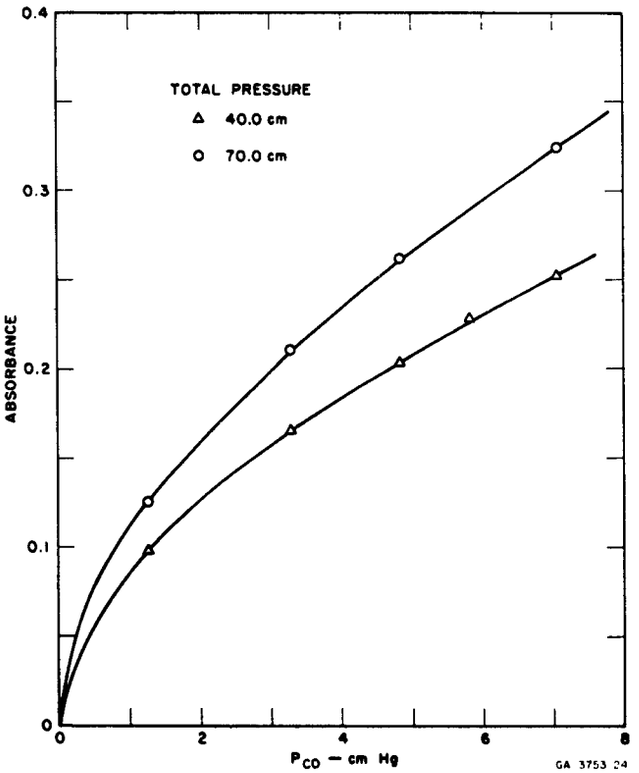

FIG. A-3 CALIBRATION CURVE FOR 2120 cm^{-1} PEAK OF CARBON MONOXIDE

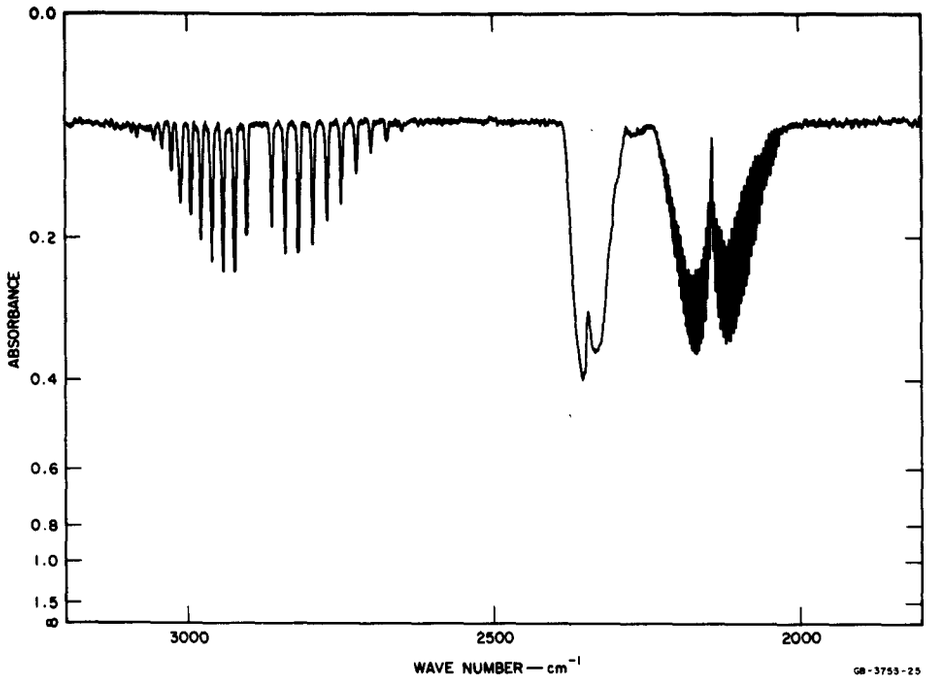

FIG. A-4 INFRARED SPECTRUM OF GASEOUS PRODUCTS OBTAINED FROM RUN 15. TOTAL PRESSURE 70.0 cm, SAMPLE PRESSURE 21.28 cm, RESOLUTION 1.8 cm^{-1}

Factors affecting the accuracy of this method are variance between the total cell pressure, between the measurement at different wave lengths, and between the sample size of the unknown gas. A statistical evaluation of these factors was made, using four different CO_2 /CO. ratios and four different sample sizes of the mixture taken for analysis at two different cell pressures. The raw data are tabulated in Table A-I; the four ratios in each group are obtained from the four possible combinations of concentrations obtained at the different wave numbers: CO_2 (2355)/CO(2170), CO_2 (2340)/CO(2170), CO_2 (2355)/CO(2120), and CO_2 (2340)/CO(2120), respectively. The data for the four ratios were subjected to analysis of variance individually, and the results from this treatment are found in Tables A-II through A-V. These data are obtained assuming that the threefold interaction is representative of the within-treatment variance (error). Significance at the 95% probability level is denoted by the mark +, 99% probability level (highly significant) by ++,

and 99.9% probability level (very highly significant) by +++. It is seen that for most ratios, the between wave-length combinations variance is significant, as is the sample-size pressure interaction variance. The calculations of the repeatability and reproducibility of the measurement for the four ratio levels are given in Table A-VI. The average repeatability is 3.5% relative.

Table A-1

RAW DATA OF STATISTICAL EVALUATION OF CO_2/CO DETERMINED

CO_2/CO Ratio taken	Total cell pressure (cm Hg)	Amount of mixture taken for analysis (cm Hg)			
		2.39	4.43	8.17	
		CO_2/CO Ratio found[a]			
0.109	40.0	0.110	0.111	0.109	
		0.126	0.114	0.120	
		0.116	0.111	0.107	
		0.132	0.115	0.118	
	70.0	0.103	0.115	0.102	
		0.120	0.116	0.113	
		0.099	0.109	0.107	
		0.115	0.111	0.119	
		2.00	4.31	6.57	8.48
0.147	40.0	0.139	0.149	0.161	0.163
		0.147	0.149	0.153	0.149
		0.154	0.144	0.155	0.172
		0.163	0.145	0.147	0.157
	70.0	0.148	0.161	0.163	0.152
		0.142	0.148	0.145	0.145
		0.154	0.165	0.168	0.159
		0.147	0.152	0.149	0.152
		2.32	4.16	6.10	7.72
0.243	40.0	0.233	0.246	0.277	0.232
		0.238	0.242	0.266	0.254
		0.222	0.238	0.268	0.279
		0.228	0.233	0.257	0.251
	70.0	0.269	0.265	0.249	0.260
		0.258	0.249	0.246	0.251
		0.260	0.232	0.248	0.258
		0.250	0.257	0.245	0.249
		2.23	4.47	5.88	
0.391	40.0	0.379	0.439	0.421	
		0.376	0.437	0.431	
		0.415	0.403	0.433	
		0.412	0.431	0.452	
	70.0	0.409	0.388	0.408	
		0.426	0.437	0.439	
		0.437	0.446	0.392	
		0.405	0.433	0.418	

[a] CO_2/CO ratio found in each group for the respective wave length combinations $CO_2(2355)/CO(2170)$, $CO_2(2340)/CO(2170)$, $CO_2(2355)/CO(2120)$, and $CO_2(2340)/CO(2120)$.

Table A-II

ANALYSIS OF VARIANCE OF
INFRARED STUDY AT A CO_2/CO RATIO OF 0.109

Source	10^4 Sum of squares	Degrees of freedom	10^4 Variance	F	Significance
Between sample size	0.45	2	0.23	1.53	-
Between total pressures	1.50	1	1.50	10.00	+
Between wavelength combinations	6.00	3	2.00	13.33	++
Sample size pressure interaction	1.47	2	0.74	4.93	-
Sample size wavelength interaction	2.14	6	0.36	2.40	-
Pressure-wavelength interaction	0.13	3	0.04	- -	-
Error	0.91	6	0.15		
Total	12.60	23	0.55		

Table A-III

ANALYSIS OF VARIANCE OF
INFRARED STUDY AT A CO_2/CO RATIO OF 0.147

Source	10^4 Sum of squares	Degrees of freedom	10^4 Variance	F	Significance
Between sample size	2.42	3	0.81	2.45	-
Between total pressures	0.00	1	0.00	- -	-
Between wavelength combinations	5.77	3	1.92	5.82	+
Sample size pressure interaction	3.54	3	1.18	3.58	-
Sample size wavelength interaction	4.28	9	0.48	1.45	-
Pressure-wavelength interaction	1.31	3	0.44	1.33	-
Error	2.99	9	0.33		
Total	20.31	31	0.66		

Table A-IV

ANALYSIS OF VARIANCE OF
INFRARED STUDY AT A CO_2/CO RATIO OF 0.243

Source	10^4 Sum of squares	Degrees of freedom	10^4 Variance	F	Signi-ficance
Between sample size	9.35	3	3.12	2.89	-
Between total pressures	2.10	1	2.10	1.94	-
Between wavelength combinations	2.35	3	0.78	- -	-
Sample size pressure interaction	25.14	3	8.38	7.75	++
Sample size wavelength interaction	11.11	9	1.23	1.14	-
Pressure-wavelength interaction	3.08	3	1.03	- -	-
Error	9.74	9	1.08		
Total	60.87	31	1.96		

Table A-V

ANALYSIS OF VARIANCE OF
INFRARED STUDY AT A CO_2/CO RATIO OF 0.391

Source	10^4 Sum of squares	Degrees of freedon	10^4 Variance	F	Signi-ficance
Between sample size	17.77	2	8.89	1.44	-
Between total pressures	.03	1	0.03	- -	-
Between wavelength combinations	12.35	3	4.12	- -	-
Sample size pressure interaction	19.30	2	9.65	1.57	-
Sample size wavelength interaction	4.56	6	0.76	- -	-
Pressure-wavelength interaction	10.99	3	3.66	- -	-
Error	36.96	6	6.16		
Total	101.96	23	4.43		

Table A-VI

REPEATABILITY AND REPRODUCIBILITY
OF CO_2/CO RATIO AT DIFFERENT LEVELS

CO_2/CO Ratio		Repeatability	Reproducibility
Taken	Found		
0.109	0.113	0.004	0.007
0.147	0.153	0.006	0.008
0.243	0.250	0.010	0.017
0.391	0.419	0.025	0.027

APPENDIX B

ANALYSIS OF GASEOUS EXHAUST PRODUCTS BY GAS-SOLID PARTITION CHROMATOGRAPHY

ANALYSIS OF GASEOUS EXHAUST PRODUCTS BY GAS-SOLID PARTITION CHROMATOGRAPHY (GSPC)

The hydrogen, nitrogen, and carbon monoxide content of the exhaust gases were determined by GSPC using a 10-foot x 1/4-inch-diameter Molecular Sieve 13X column at 28°C, a helium flow rate of 31.9 ml/min, and a filament current of 280 ma. A measured amount of sample gas was introduced into the evacuated 1.00-ml sampling valve and then transferred to the helium gas stream at the top of the column. The chromatogram was obtained and the areas of the hydrogen, oxygen, nitrogen, and carbon monoxide peaks were determined. For nitrogen and carbon monoxide, the percent of each in the sample was determined by the following equation:

$$\%X_i = \frac{100A_i}{Pf_i} \qquad \text{(B-1)}$$

where A_i is the area of the component, f_i is the calibration factor, and P is the sample pressure. For nitrogen a correction for the air in the sample is applied

$$\%N_2 = \frac{(A_{N_2} - 3.76A_{O_2})}{Pf_{N_2}} 100 \qquad \text{(B-2)}$$

For hydrogen, the calibration curve (Fig. B-1) was used.

Carbon dioxide was determined in a similar manner using a 1-1/2 foot x 1/4-inch-diameter silica gel column, at 28°C, a helium flow rate of 60.0 ml/min, and a filament current of 295 ma. The measured calibration factors for these gases are listed in Table B-I in units independent of flow rate but dependent on filament current. The instrument area response was 5893 disc integrator counts/mv-min.

Table B-II lists the characteristics of these exhaust products with the Molecular Sieve 13X column.

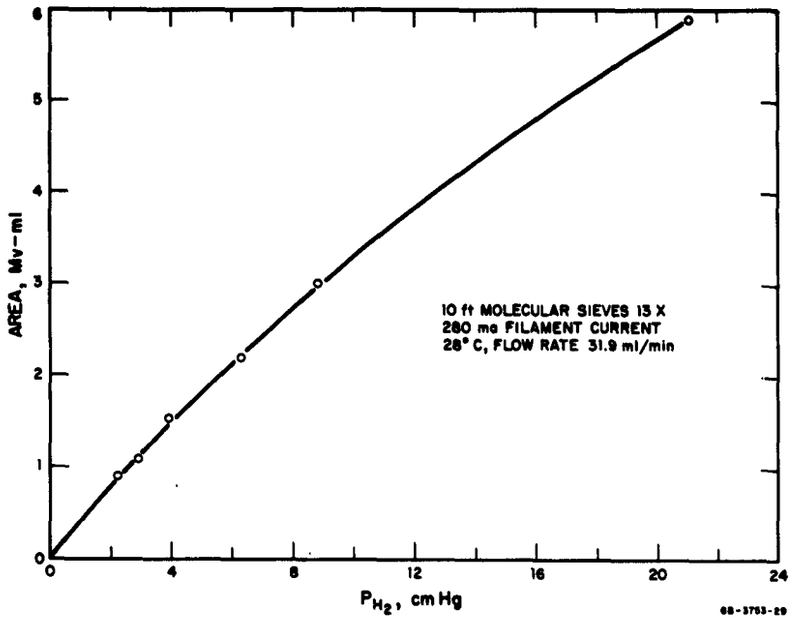

FIG. B-1 CALIBRATION CURVE: PARTIAL PRESSURE OF HYDROGEN AS A FUNCTION OF PEAK AREA

Table B-I

GSPC CALIBRATION FACTORS FOR EXHAUST GASES

Gas	Filament Current ma	f_i mv-ml/cm Hg
CO	280	13.93
N_2	280	13.34
CO_2	295	27.16

Table B-II

GAS CHROMATOGRAPHIC CHARACTERISTICS OF SOME ROCKET EXHAUST COMPONENTS USING A 10-FOOT, 1/4-INCH DIAMETER, MOLECULAR SIEVE 13X COLUMN

Exhaust Component	Relative Retention Time	Theoretical Plates
Hydrogen	0.34	- -
Oxygen	0.65	1160
Nitrogen	1.00	1290
Carbon Monoxide	1.98	920

APPENDIX C

MASS SPECTROMETRIC ANALYSIS OF GASEOUS EXHAUST PRODUCTS

MASS SPECTROMETRIC ANALYSIS OF GASEOUS EXHAUST PRODUCTS

The mass spectrometer used for these analyses was a Consolidated Electrodynamics Corporation Model 21-103C equipped with a rhenium filament and a heated inlet system (100°C).

The hydrogen chloride- and water-free gas samples were introduced into the inlet system at a pressure of the order of 100 microns, and masses were scanned from m/e 2 to m/e 46, using an ionizing current of 10.5 microamperes. (A few trial runs to m/e 130 indicated that only traces of pyridine were carried over from the preliminary pyridine neutralization.)

The vol-% (or mol-%) of the individual gases present in the exhaust-gas mixture was calculated by the following equation:

$$\text{Vol-\%} = \frac{100\ d}{spi}$$

where d = divisions (or peak height) of component at a characteristic m/e

s = sensitivity (divisions/micron/microampere) of the component at the characteristic m/e

i = ionizing current, in microamperes

p = sample pressure, in microns.

The gases used as standards for these determinations were of at least 99.8% purity after treatment in this laboratory; the sensitivities at characteristic m/e values are given in the following table:

Table C-I

MASS SPECTROMETER SENSITIVITIES OF GASEOUS EXHAUST PRODUCTS

Gas	m/e	Sensitivity* (div/micron/microamp)
H_2	2	0.843
H_2O	18	1.080
N_2	28	1.680
CO	28	1.672
A	40	2.352
CO_2	44	1.885

* Reference standard: n-decane at m/e 43, sensitivity = 364

The determination of hydrogen, oxygen, argon, and carbon dioxide in the samples was straightforward because the peak height of each of these gases at characteristic m/e values was unaffected by contributions from other gases in the mixture. However, the determination of carbon monoxide in the presence of nitrogen is a well-known mass spectrometric problem. Both gases have a molecular-ion mass of 28, more precisely, 28.016 (N_2) and 28.01 (CO). A resolving power of one part per 5000 is necessary to separate these masses; under optimum operating conditions, good resolution of only one part per 500 can be obtained with the Model 21-103C. In general, the analysis of a multicomponent system can be achieved by solution of simultaneous equations involving peak heights (and sensitivities) for at least two m/e values; however, carbon monoxide and nitrogen have the same sensitivities for the parent ions (see Table C-I)and the other ions formed by their fragmentation are of such low sensitivity that solution of simultaneous equations yields results that are likely to be in error. Hence, the mol ratio of carbon monoxide to nitrogen observed by gas chromatography was applied to the total carbon monoxide-nitrogen mol percent (determined mass spectrometrically) to obtain the mol percent CO and N_2.

APPENDIX D

DETERMINATION OF CARBON, WATER, AND METALLIC ALUMINUM CONTENT OF SOLID EXHAUST PRODUCTS

DETERMINATION OF CARBON, WATER, AND METALLIC ALUMINUM CONTENT OF SOLID EXHAUST PRODUCTS

Apparatus

A combustion furnace capable of heating to 1100°C is required, and a source of water-free oxygen. Porcelain sample boats for semi-micro combustion, micro gas absorption tubes, and a semi-micro balance are also utilized. A typical setup is shown in Fig. D-1.

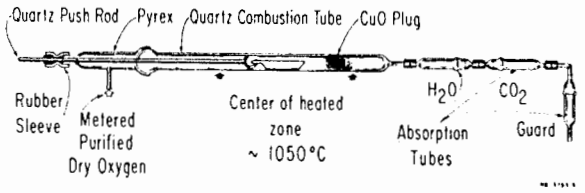

FIG. D-1 COMBUSTION TRAIN SET-UP FOR DETERMINATION OF METALLIC ALUMINUM, CARBON, AND WATER IN SOLID EXHAUST PRODUCT

Reagents

Tetrasodium pyrophosphate, ($Na_4P_2O_7$) prepared by maintaining reagent-grade disodium hydrogen orthophosphate (Na_2HPO_4) at 500°C for several hours. Store the ignited material in a tightly-stoppered bottle.

Dry oxygen

Pure alumina, (Al_2O_3) ignited, powdered

Aluminum, 99.9% pure, powder.

Procedure

Transfer about 1.0 g sodium pyrophosphate flux to a porcelain boat. Weigh the flux and boat accurately (to ±0.01 mg), and add 0.1-0.15 g of sample. Mix the contents of the boat thoroughly by use of a wire or small spatula and again weigh the boat and contents to the nearest 0.01 mg. Obtain the tare weight of a magnesium perchlorate

(anhydrone) and an ascarite absorption tube (to the nearest 0.01 mg). Attach the absorption tubes in the order shown in Fig. D-1, place the boat and contents in the combustion furnace tube, attach the oxygen line, maintain an oxygen flow rate of 5-10 ml/min and heat at 1050°C for three hours. Turn off furnace, allow the sample to cool to about 500°C, and then transfer the boat and contents and the two absorption tubes to a desiccator. Cool to room temperature and weigh. Repeat the above procedure without a sample to determine the flux-blank for carbon dioxide, water, and flux weight loss.

Calculations

Calculate the percent carbon, water, and metallic aluminum in the sample as follows:

$$\text{Percent carbon} = 27.3 \frac{(W_1 - W_3)}{W_S}$$

$$\text{Percent water} = 100 \frac{(W_2 - W_4)}{W_S}$$

$$\text{Percent aluminum} = 112.5 \frac{(\delta + W_2 + 0.273\, W_1)}{W_S}$$

where

W_S = weight of sample, mg

W_1 = increase in weight of ascarite absorption tube for sample determination, mg

W_2 = increase in weight of anhydrone absorption tube for sample determination, mg

W_3 = increase in weight of ascarite absorption tube for blank run, mg

W_4 = increase in weight of anhydrone absorption tube for blank run, mg

δ = increase in weight of combustion boat for sample determination, mg.

Discussion

Results typical of those obtainable by this method are found in Table D-I.

Table D-1

TYPICAL RESULTS OF COMBUSTION ANALYSIS
OF ALUMINUM-ALUMINA MIXTURES
AS A FUNCTION OF COMBUSTION

Period at 1100°C, Weight of Aluminum, and the Weight Ratio of Flux to Sample

Combustion Period, min	Wt of Al in Sample, mg	Wt Flux Wt Sample	Percent Aluminum		
			Taken	Found	Difference
120	2.73	2.11	0.80	0.79	-0.01
120	2.54	4.99	1.43	1.61	+0.18
150	3.02	2.28	1.04	0.95	-0.09
150	4.93	2.21	1.79	1.69	-0.10
150	5.60	4.51	3.40	3.34	-0.06
150	12.42	2.14	5.06	4.37	-0.69
150	29.41	3.21	13.28	8.30	-4.98
240	15.75	3.53	7.74	7.10	-0.64

APPENDIX E

SOLUTION OF SOLID EXHAUST PRODUCT

SOLUTION OF SOLID EXHAUST PRODUCT

In an agate mortar, grind the sample until it passes through a 150 mesh (104μ) sieve. Transfer an accurately weighed (to 0.1 mg) portion of sample of about 0.4 g to a platinum crucible which contains about 1 g of potassium bisulfate and mix well. Add an additional 3 to 4 g of potassium bisulfate and heat the crucible and contents gently with a Meeker burner until the contents are molten, then increase the heat until the crucible is dull red in color, and maintain that temperature for 20 minutes. If it appears that the fusion is incomplete, cool the crucible, add about 2 ml of reagent-grade sulfuric acid and repeat the fusion process for 10 minutes. When the fusion is complete, cool the crucible partially and transfer the contents to a 250-ml beaker. Add 20 ml of reagent-grade sulfuric acid and disperse the fusion mixture with the aid of a stirring rod. Heat the suspension until sulfur trioxide fumes are given off, then cool, and dissolve the mixture with 150 ml of water. Solution of the mixture may require prolonged (overnight) stirring. Quantitatively transfer the solution to a 250-ml volumetric flask or one of desired size and fill to the mark. Calculate the concentration of sample in the volumetric flask, C_s, as follows:

$$C_s = \frac{W}{V}$$

where W = weight of sample, mg
and V = volume of volumetric flask, ml.

APPENDIX F

VOLUMETRIC DETERMINATION OF ALUMINA

VOLUMETRIC DETERMINATION OF ALUMINA

Reagents

Aluminum metal, foil 99.9% W/W min. Alcoa

Reagent-grade hydrochloric acid

Disodium ethylenediaminetetraacetate solution, 0.1 M

Dissolve approximately 35-40 g of reagent-grade disodium ethylenediaminetetraacetate dihydrate in water and dilute to one liter in a volumetric flask. Standardize the solution by titration of a 25-ml aliquot of 0.05 M standard zinc chloride solution using the procedure described below. Carry out a blank titration (with no zinc chloride solution) with zinc acetate solution. Calculate the concentration of the disodium ethylenediaminetetraacetate solution as follows:

$$M_E = \frac{V_z M_z}{(1 - \frac{v_s}{v_b}) V_E}$$

where V_z = volume of standard zinc chloride solution, ml

M_z = concentration of standard zinc chloride solution, moles/liter

V_E = volume of disodium ethylenediaminetetraacetate solution, ml

v_s = volume of zinc acetate solution required for titration of the sample, ml

v_b = volume of zinc acetate solution required for blank titration, ml.

Zinc Chloride solution, 0.05 M, primary standard

Transfer an accurately weighed portion (nearest mg) of approximately 3.0-3.5 g of reagent-grade zinc metal into a 100-ml beaker. Add 20 ml of reagent-grade hydrochloric acid, assist solution with heat, and allow the zinc to dissolve completely. Quantitatively transfer the contents of the beaker to a one-liter volumetric flask and then fill to

the mark. The molar concentration of the solution is calculated as follows:

$$\text{concentration zinc chloride} = M_z = \frac{\text{wt zinc metal}}{65.38}$$

Zinc Acetate solution, 0.05 M

Dissolve about 11 g of reagent-grade zinc acetate, $Zn(C_2H_3O_2)_2 \cdot 2H_2O$ in water, add 1 ml of glacial acetic acid, and dilute to 1 liter with water in a 1-liter volumetric flask. Calculate the concentration of the solution from titrations made in the standardization of the disodium ethylenediaminetetraacetate solution as follows:

$$\text{concentration of zinc acetate} = M_A = \frac{M_E V_E}{V_b}$$

Dithizone Indicator solution

Dissolve 25 mg of dithizone in 100 ml of ethanol. This solution is unstable and must be freshly prepared every two days.

Ethanol, 95% V/V

Acetate-Acetic Acid buffer

Dissolve 77 g of reagent grade ammonium acetate and 59 ml of glacial acetic acid (98% W/W) in sufficient water to make one liter.

Aluminum Chloride solution, 0.1 M

Transfer an accurately weighed portion (nearest mg) of about 3 g of aluminum foil to a 100-ml beaker. Add 20 ml of reagent-grade hydrochloric acid to a 100-ml beaker, assist solution with heat, and allow the aluminum to dissolve completely. Quantitatively transfer the contents of the beaker to a one-liter volumetric flask and then fill to the mark. The molar concentration of the solution is calculated as follows:

$$\text{concentration aluminum chloride} = M_{Al} = \frac{\text{wt aluminum foil}}{26.97}$$

Procedure

Transfer an aliquot of the aluminum solution which is to be examined into a 250-ml Erlenmeyer flask. The size of the aliquot should be sufficient to transfer about 1.2 mmole of aluminum. From a buret add 25.00 ml of the disodium ethylenediaminetetraacetate solution. Add 10 ml of acetate-acetic acid buffer and then double the volume in the flask with ethanol. For every 50 ml of solution in the flask add 1 ml of dithizone indicator solution. The end point color change is a sharp one-drop change from green to pink.

Calculation

Calculate the percent alumina in the sample as follows:

$$\%Al_2O_3 = \frac{5097\ (V_e M_e - M_a v_s)}{C_s v_a} - 1.927\ (\%Al)$$

where

V_e = volume of disodium ethylenediaminetetraacetate solution used, ml

M_e = concentration of disodium ethylenediaminetetraacetate solution, moles/liter

M_a = concentration of zinc acetate solution, moles/liter

v_s = volume of zinc acetate solution required for titration of sample, ml

v_a = volume of aliquot of sample solution taken, ml

C_s = concentration of sample, mg/ml (see Appendix E)

%Al = percent metallic aluminum in the solid exhaust product (see Appendix D).

Discussion

Results typical of those obtainable by this method are found in Table F-1.

Table F-I

TYPICAL RESULTS OF ALUMINUM DETERMINATION

Aluminum Taken mmole	Aluminum Found mmole	Error
0.6223	0.6280	+0.0057
0.6223	0.6223	0.0000
0.6223	0.6213	-0.0010
0.6223	0.6258	+0.0035
Average	0.6244	+0.0021
Standard Deviation	0.0030	
Coefficient of Variation	0.48 %	
0.05602	0.05596	-0.00003
0.05602	0.05674	+0.00072
0.05602	0.05685	+0.00083
0.05602	0.05596	-0.00003
0.05602	0.05627	+0.00025
0.05602	0.05617	+0.00015
Average	0.05633	+0.00031
Standard Deviation	0.000386	
Coefficient of Variation	0.68 %	

APPENDIX G

POLAROGRAPHIC ANALYSIS OF MINOR METAL CONSTITUENTS IN SOLID EXHAUST PRODUCTS

POLAROGRAPHIC ANALYSIS OF MINOR METAL CONSTITUENTS IN SOLID EXHAUST PRODUCTS

Minor metal constituents in the solid exhaust product are determined polarographically in the following manner.

Determination of Iron

An aliquot of the fusion mixture solution Appendix E is transferred to a polarographic cell. The contents of the cell are deaerated with a stream of oxygen-free nitrogen for 15 minutes, and a polarogram is run from +0.2 to -1.0v vs. S. C. E. The limiting current at -0.2v is corrected for its residual current component and the concentration of iron in the solution is determined from the calibration curve presented in Fig. G-1.

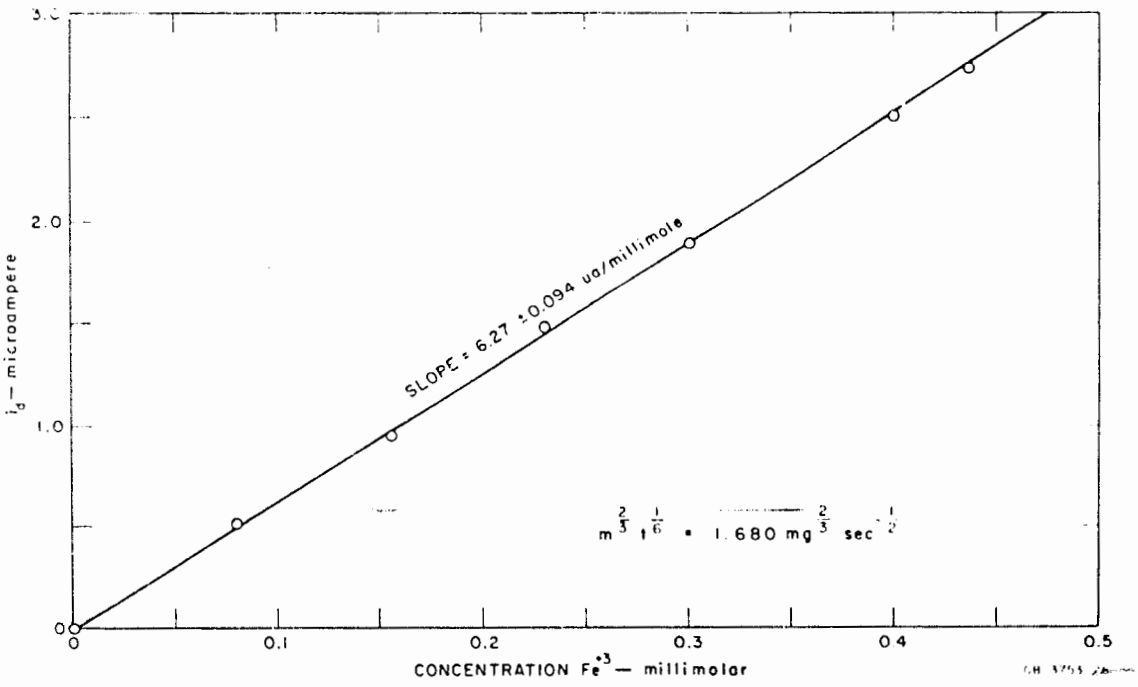

FIG. G-1 DIFFUSION CURRENT vs. CONCENTRATION FOR Fe^{+3} IN SULFATE-BISULFATE MEDIA AT -0.2 VOLTS vs. S.C.E.

The percent iron in the solid sample is calculated as percent ferric oxide as follows:

$$\text{Percent } Fe_2O_3 = \frac{(7.985)\left(\frac{V_t}{V_A}\right)M}{C_s}$$

where V_t/V_A = ratio of total volume of polarographic sample to the volume of aliquot taken.

M = concentration of iron found from calibration curve, millimolar

C_s = concentration of sample in fusion solution, mg/ml, (see Appendix E)

Presence of Zinc

The presence of zinc can be verified by observation of a polarographic wave with a half-wave potential at -0.15v vs. S.C.E. The maximum concentration of zinc which can be detected with this experimental setup is 1.9×10^{-5} M. This concentration of zinc has a diffusion current of 0.035 μa at -0.2v. If zinc is present at this low concentration level, it would appear to enhance the iron wave to an extent of 5×10^{-6} M or 0.005% Fe_2O_3 in a typical sample. This error can be alternatively expressed as the maximum quantity of zinc oxide that could be present in a sample and not give rise to a zinc wave, 0.2% ZnO.

APPENDIX H

SPECTROPHOTOMETRIC DETERMINATION OF TITANIUM IN SOLID ROCKET EXHAUST PRODUCTS

SPECTROPHOTOMETRIC DETERMINATION OF TITANIUM IN SOLID ROCKET EXHAUST PRODUCTS

The product of the bisulfate fusion is dissolved in a small amount of sulfuric acid (Appendix E). An aliquot is transferred to a volumetric flask. Five milliliters of 30% w/w hydrogen peroxide is added and the flask is filled to the mark. After mixing the solution thoroughly, a sufficient quantity is transferred to fill a 10-cm optical cell, and its absorbance at 400 mμ is measured with respect to a sample blank. The percent titanium is calculated from the pertitanic color by the following:

$$\%Ti = \frac{4.79V_t}{abV_a C_s} A$$

where V_t = volume of volumetric flask, ml

V_a = volume of aliquot, ml

a = absorbancy index, liter/mole-cm

b = optical path length, cm

A = absorbance at 400 mμ

C_s = concentration of solid exhaust sample in original fusion solution, mg/ml (see Appendix E)

A plot of absorbance as a function of concentration is given in Fig. H-1. This curve was obtained using a 1.0-cm optical cell. Deviations from the Lambert-Beer-Bouger law occur at absorbance values greater than 0.9.

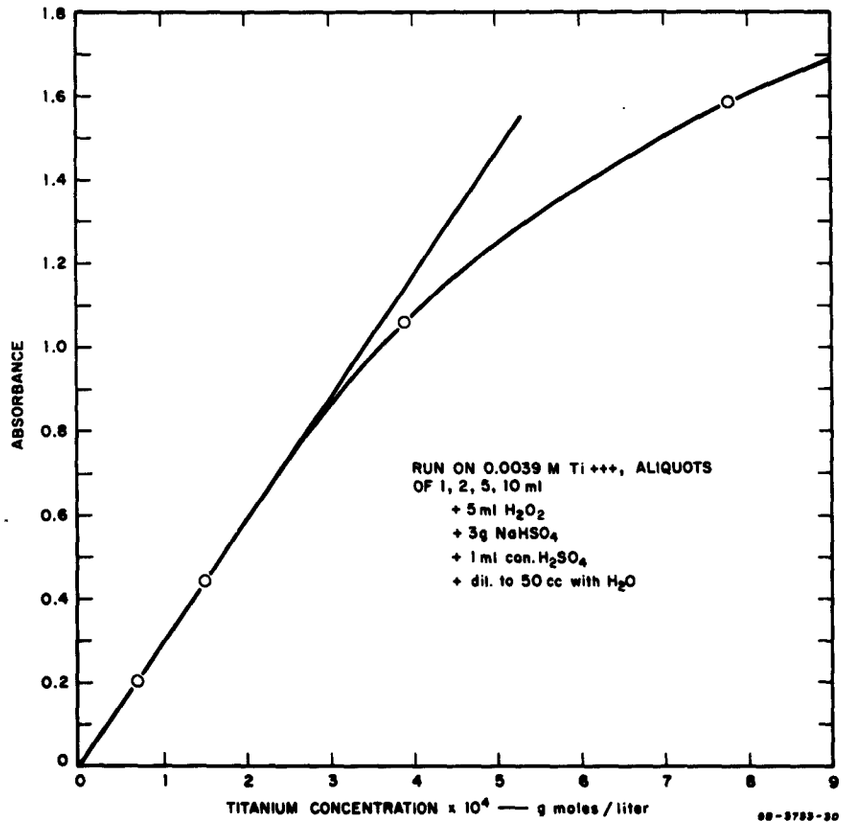

FIG. H-1 BEER'S LAW CURVE FOR TITANIUM DETERMINATION, b = 1.00 cm

APPENDIX I

SPECTROPHOTOMETRIC DETERMINATION OF TANTALUM IN SOLID EXHAUST PRODUCTS (PEROXIDE METHOD)

SPECTROPHOTOMETRIC DETERMINATION OF TANTALUM IN SOLID EXHAUST PRODUCTS (PEROXIDE METHOD)

The peroxy complex of tantalum in 96% sulfuric acid, $TaO_4^{\equiv}$, exhibits absorption in the ultraviolet spectrum, with an absorption peak at 286 mμ. This property is utilized in a spectrophotometric determination of tantalum. Because of the complex nature of the solid propellant exhaust samples, which contained other materials absorbing near the peroxy-tantalum peak, special sample preparation and blank determinations were necessary.

Special Reagents

Pure tantalum metal

Reagent grade hydrofluoric acid, 50-52% W/W

Reagent grade sulfuric acid, 95 + % W/W

Hydrogen peroxide-sulfuric acid mixture, 1:9 V/V--reagent grade hydrogen peroxide (30%): reagent grade sulfuric acid.

Preparation of Standard Peroxytantalum Solutions for the Beer's Law Curve

Transfer a weighed quantity of tantalum into a platinum evaporating dish, add 10 ml of hydrofluoric acid, and if necessary, heat. After solution, add 20 ml of sulfuric acid to the dish, and heat the dish and contents until dense sulfuric trioxide fumes evolve. Allow the dish and contents to come to room temperature and, with sulfuric acid, transfer the contents quantitatively into a volumetric flask of the desired size. Fill the flask to the mark with sulfuric acid and mix well.

Transfer an aliquot of the standard tantalum solution into a 50-ml volumetric flask, add a 10-ml aliquot of the hydrogen peroxide-sulfuric acid solution to the flask, and mix the contents well. Cool the flask and contents to room temperature and dilute to volume with sulfuric acid.

Prepare a peroxide blank by transferring a 10-ml aliquot of the hydrogen peroxide-sulfuric acid solution into a 50-ml volumetric flask which contains about 30 ml of sulfuric acid. Mix the contents well and

cool the flask to room temperature. Fill the flask to the mark with sulfuric acid and mix well.

Transfer solutions of the peroxytantalic ion and the peroxide blank to matched 1-cm ultraviolet absorption cells and record the absorbance of the peroxytantalic ion vs. the peroxide reference at 286 mμ. Solutions prepared in the above manner gave the calibration curves (Fig. I-1), with an absorbancy index of 1010 liter/mol-cm.

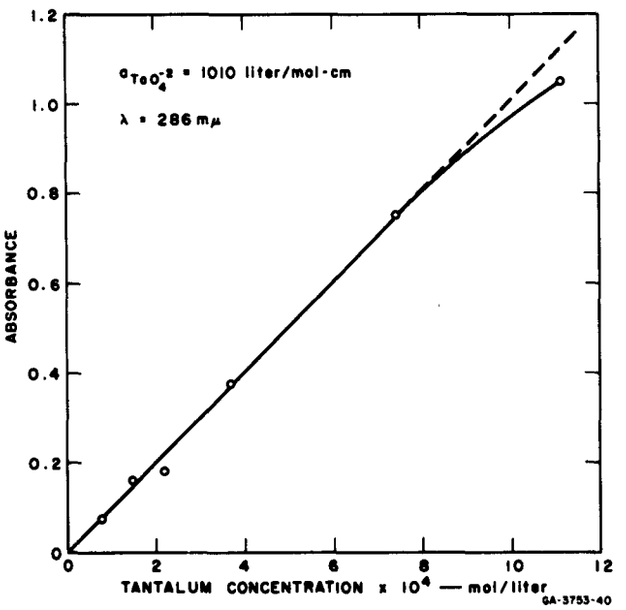

FIG. I-1 CALIBRATION CURVE FOR THE SPECTROPHOTOMETRIC DETERMINATION OF TANTALUM

Determination of Tantalum in Solid Exhaust Samples

Because iron is present in the exhaust sample and absorbs at 286 mμ it is necessary to prepare a separate sample blank without peroxide, determine its absorbance, and then correct for its contribution to the peroxytantalic absorbance.

Transfer two 1/10 aliquots of the diluted bisulfate fusion mixture (Appendix E) into separate platinum evaporating dishes. Evaporate the contents of the dishes until dense sulfur trioxide fumes evolve.

Permit the dishes and contents to cool, and, to each dish add 5 ml of hydrofluoric acid, assist solution of the hydrous tantalic oxide with heat, (if necessary) add 20 ml of sulfuric acid, and heat until dense sulfur trioxide fumes re-appear. Allow the dishes and contents to come to room temperature, and if a precipitate is observed, repeat the addition of hydrofluoric acid and evaporation to sulfur trioxide fumes until no precipitate is seen. Quantitatively transfer the contents of the dishes to separate 50 ml volumetric flasks with sulfuric acid. Transfer a 10-ml aliquot of hydrogen peroxide-sulfuric acid solution into one flask and to the other add exactly 1 ml of water. Cool the flasks to room temperature, fill each flask to the mark with sulfuric acid and mix well. Prepare a peroxide reference solution as described in the preceding section and prepare a blank reference solution by transferring 1 ml of water into a 50-ml volumetric flask which contains about 30-40 ml of sulfuric acid; cool the flask to room temperature and fill to the mark with sulfuric acid and mix well.

Transfer portions of the four solutions to respective matched 1.00-cm silica cells; and, at 286 mμ measure the absorbance of the peroxy tantalic ion against the peroxide reference solution, and the sample blank against the sample blank reference.

Calculate the percent tantalum oxide in the sample as follows:

$$\%Ta_2O_5 = \frac{2188\ (A_p - A_b)}{C_s}$$

where A_p = absorbance of peroxy tantalic solution vs a peroxide blank at 286 mμ obtained with matched 1.00-cm silica cells

A_b = absorbance of the sample blank vs. a sample blank reference at 286 mμ obtained with matched 1.00-cm silica cells

C_s = concentration of solid exhaust sample in original fusion solution mg/ml

APPENDIX J

SPECTROPHOTOMETRIC DETERMINATION OF TANTALUM IN SOLID EXHAUST PRODUCTS (METHYL VIOLET METHOD)

SPECTROPHOTOMETRIC DETERMINATION OF TANTALUM IN SOLID EXHAUST PRODUCTS (METHYL VIOLET METHOD)

The methyl violet complex of tantalum exhibits absorption in the visible spectrum, with an absorption peak at 600 mμ. The visible spectrum of this complex is shown in Fig. J-1. This property is utilized in the spectrophotometric determination of tantalum in the solid exhaust product.

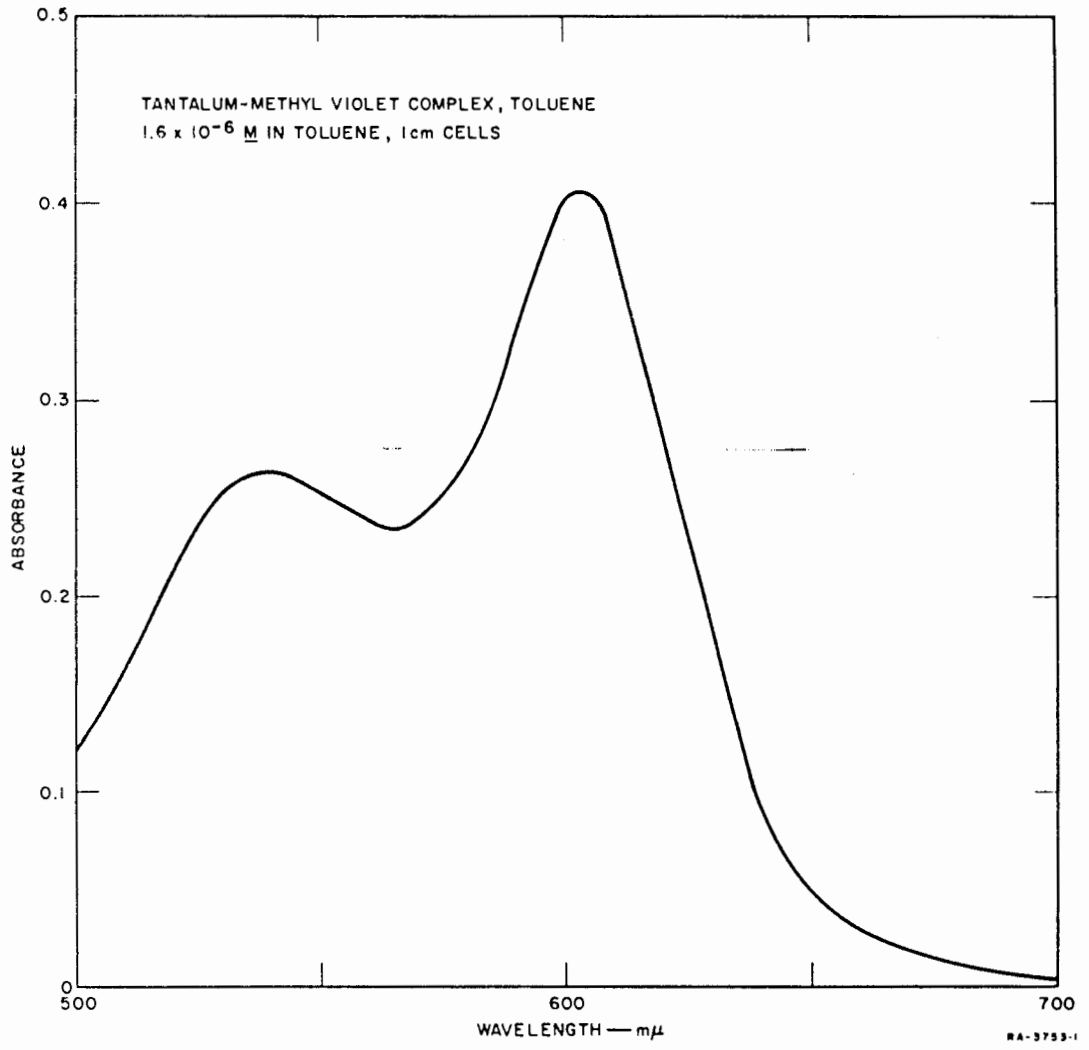

FIG. J-1 ABSORPTION CURVE OF TANTALUM-METHYL VIOLET COMPLEX

Special Reagents

Reagent grade hydrofluoric acid, 50-52% W/W
Reagent grade sulfuric acid, 95 + % W/W
0.03% W/V Methyl violet indicator in water
0.3% W/V Methyl violet indicator in 1:1 V/V water-ethanol
3M Sodium hydroxide solution
Reagent grade sodium hydroxide pellets
Reagent grade toluene
60% W/V Potassium fluoride solution

Procedure

Transfer a 1-ml aliquot of the diluted bisulfate fusion mixture (Appendix E) into a platinum evaporating dish and evaporate the contents to dryness. Permit the dishes and contents to cool, add 2 ml of hydrofluoric acid, assist solution of the hydrous tantalic oxide with heat (if necessary), add 5 ml of sulfuric acid, and heat until dense sulfur trioxide fumes appear. Allow the dishes and contents to come to room temperature, and if a precipitate is observed, repeat the addition of hydrofluoric acid and evaporation to sulfur trioxide fumes until no precipitate is seen.

Quantitatively transfer the contents of the evaporating dish into a 150-ml beaker which contains 15 ml of potassium fluoride solution. To the beaker add 1 ml of 0.03% methyl violet indicator and sufficient water to bring the volume to approximately 90 ml. Mix the contents of the beaker and adjust the pH of the solution with sodium hydroxide pellets until its color becomes blue-green. Then, add 3 M sodium hydroxide until the solution just turns blue. Quantitatively transfer the contents of the beaker to a 250-ml extraction funnel, and dilute to a total volume of approximately 120 ml with water. Add 5 ml of 0.3% methyl violet solution and 5 to 7 ml of toluene. Invert the extraction funnel a minimum of 50 times, allow the layers to separate, and transfer the organic layer to a 100-ml volumetric flask. Repeat the extraction steps 10 times or until the toluene layer is colorless. Fill the volumetric flask to the mark with toluene, mix its contents well, and transfer a portion of the

solution to a 1.00-cm optical cell. The methyl violet-tantalum fluoride solutions are not stable for long periods before extraction; hence extraction should commence as soon as the methyl violet is added. The methyl violet complex is stable in toluene for two hours.

Calculate the percent tantalum oxide in the solid product as follows:

$$\% Ta_2O_5 = 0.07594 \frac{V_f}{V_a} \frac{A_i}{C_s}$$

where

A_i = absorbance of methyl violet complex at 600 mμ
V_f = volume of volumetric flask, ml (100 ml)
V_a = volume of aliquot taken for analysis
C_s = concentration of solid exhaust sample in original fusion mixture, mg/ml.

APPENDIX K

PLANS FOR EXHAUST SAMPLER USED FOR CALAVERAS TEST SITE MOTOR FIRINGS

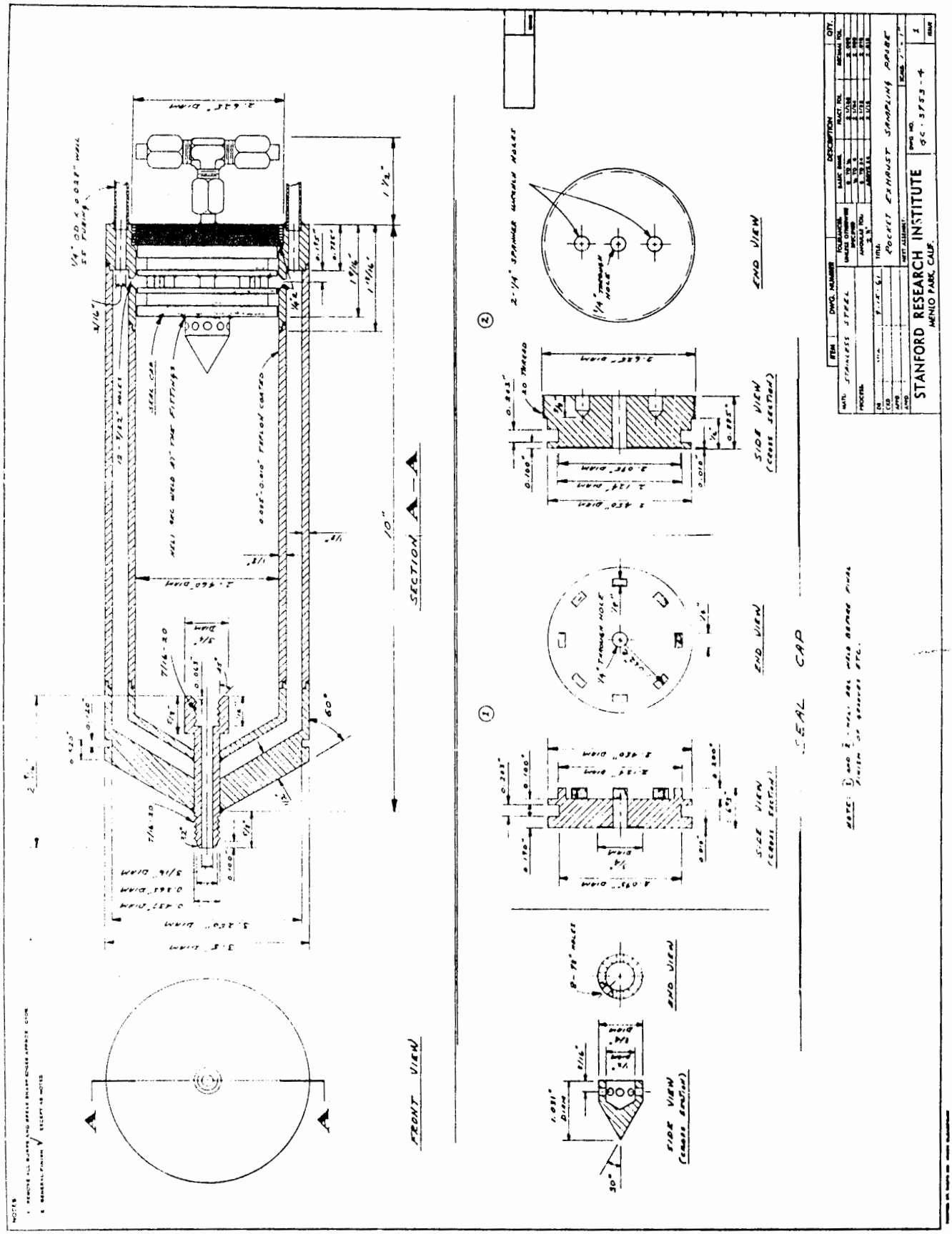

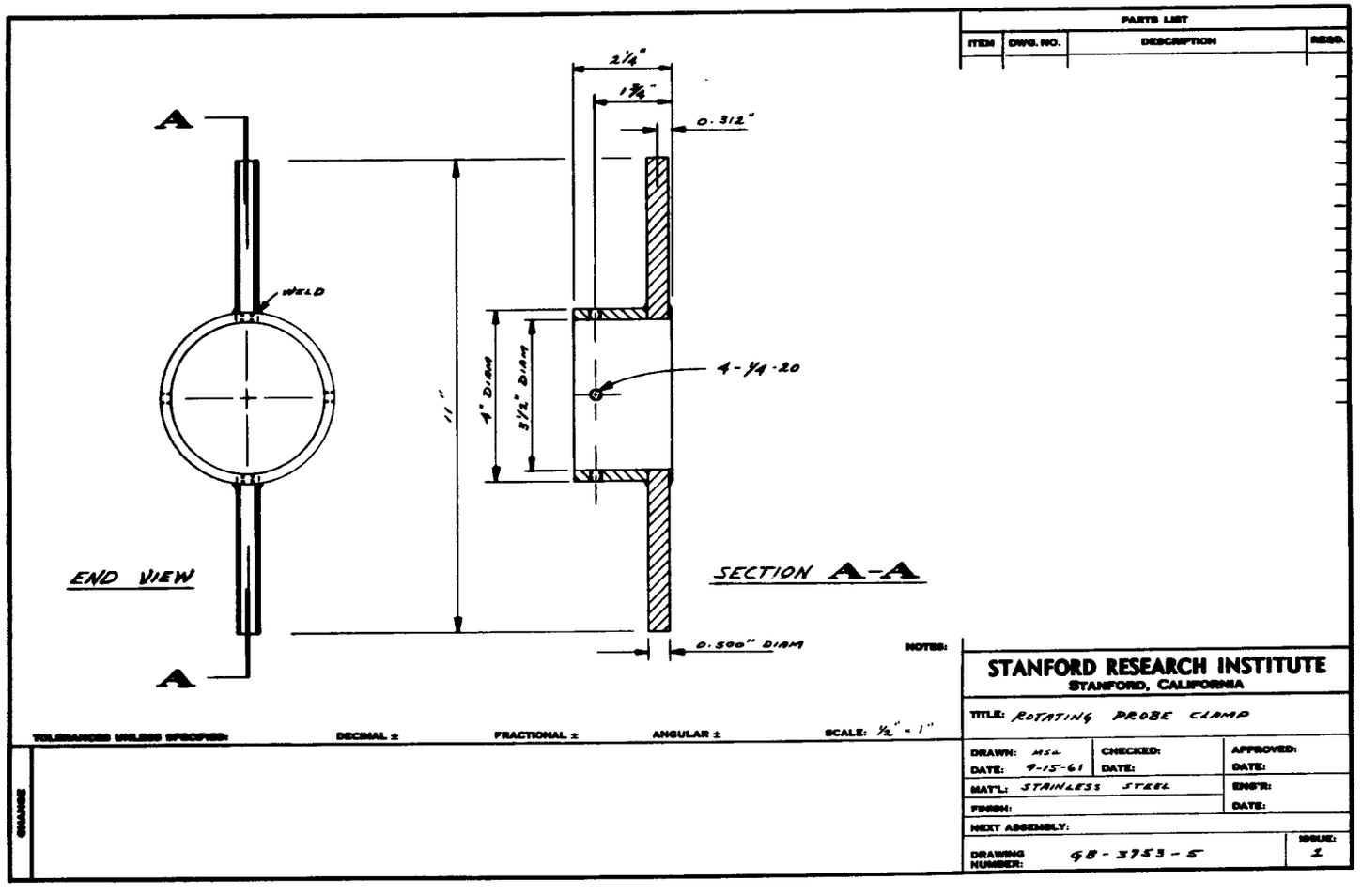
A
A
WELD
END VIEW
2¼"
1¾"
0.312"
11"
4" DIAM
3½" DIAM
4-¼-20
0.500" DIAM
SECTION A-A
PARTS LIST
ITEM
DWG. NO.
DESCRIPTION
REQD.
NOTES:
STANFORD RESEARCH INSTITUTE
STANFORD, CALIFORNIA
TITLE: ROTATING PROBE CLAMP
DRAWN: MSA
DATE: 9-15-61
CHECKED:
DATE:
APPROVED:
DATE:
MAT'L: STAINLESS STEEL
FINISH:
ENG'R:
DATE:
NEXT ASSEMBLY:
DRAWING NUMBER: 68-3753-5
ISSUE: 1
TOLERANCES UNLESS SPECIFIED: DECIMAL ± FRACTIONAL ± ANGULAR ± SCALE: ½" = 1"
CHANGE

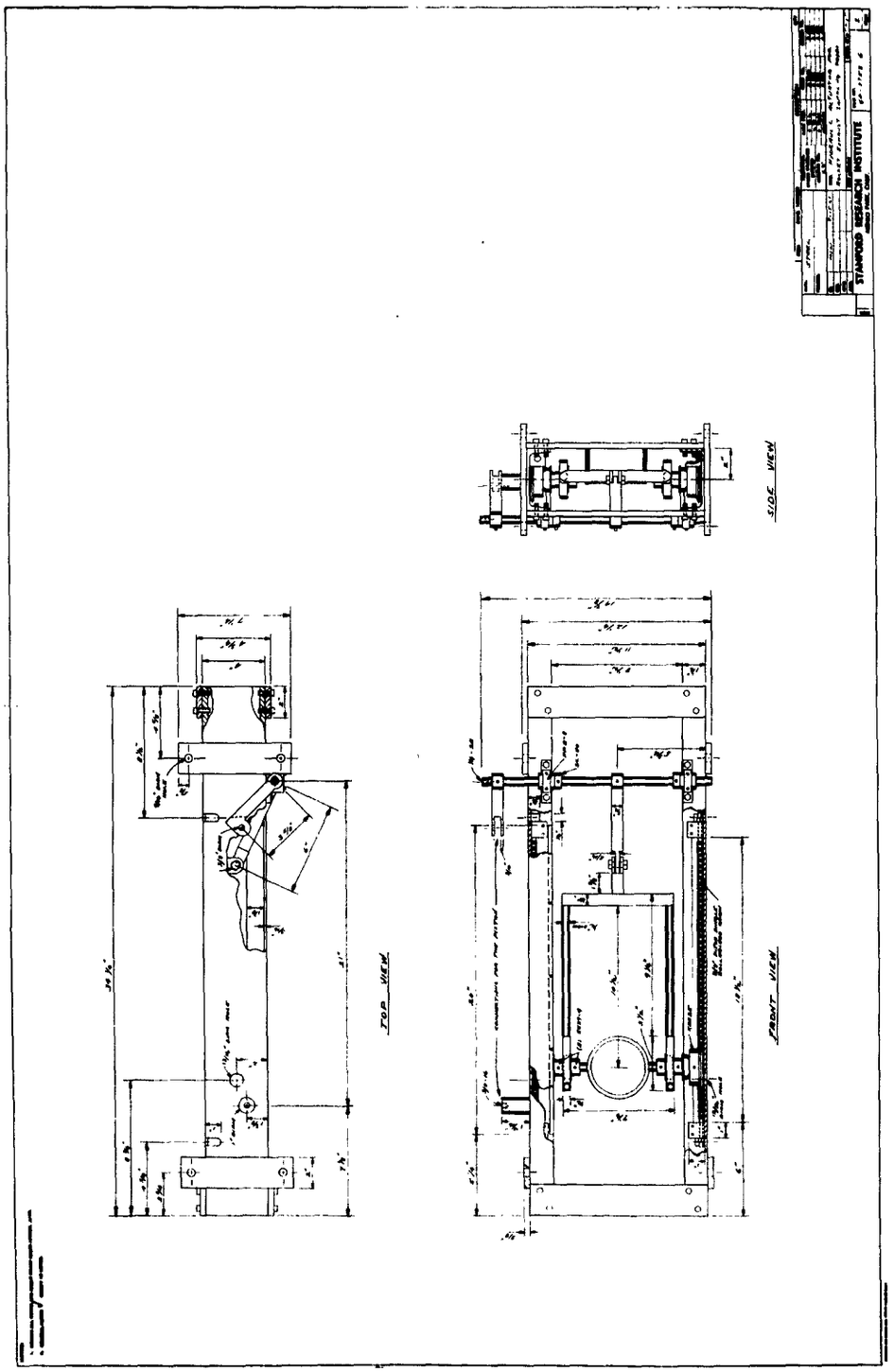
STANFORD RESEARCH INSTITUTE
SIDE VIEW
TOP VIEW
FRONT VIEW

APPENDIX L

PLANS FOR EXHAUST SAMPLER USED FOR AEROJET-GENERAL MOTOR FIRINGS

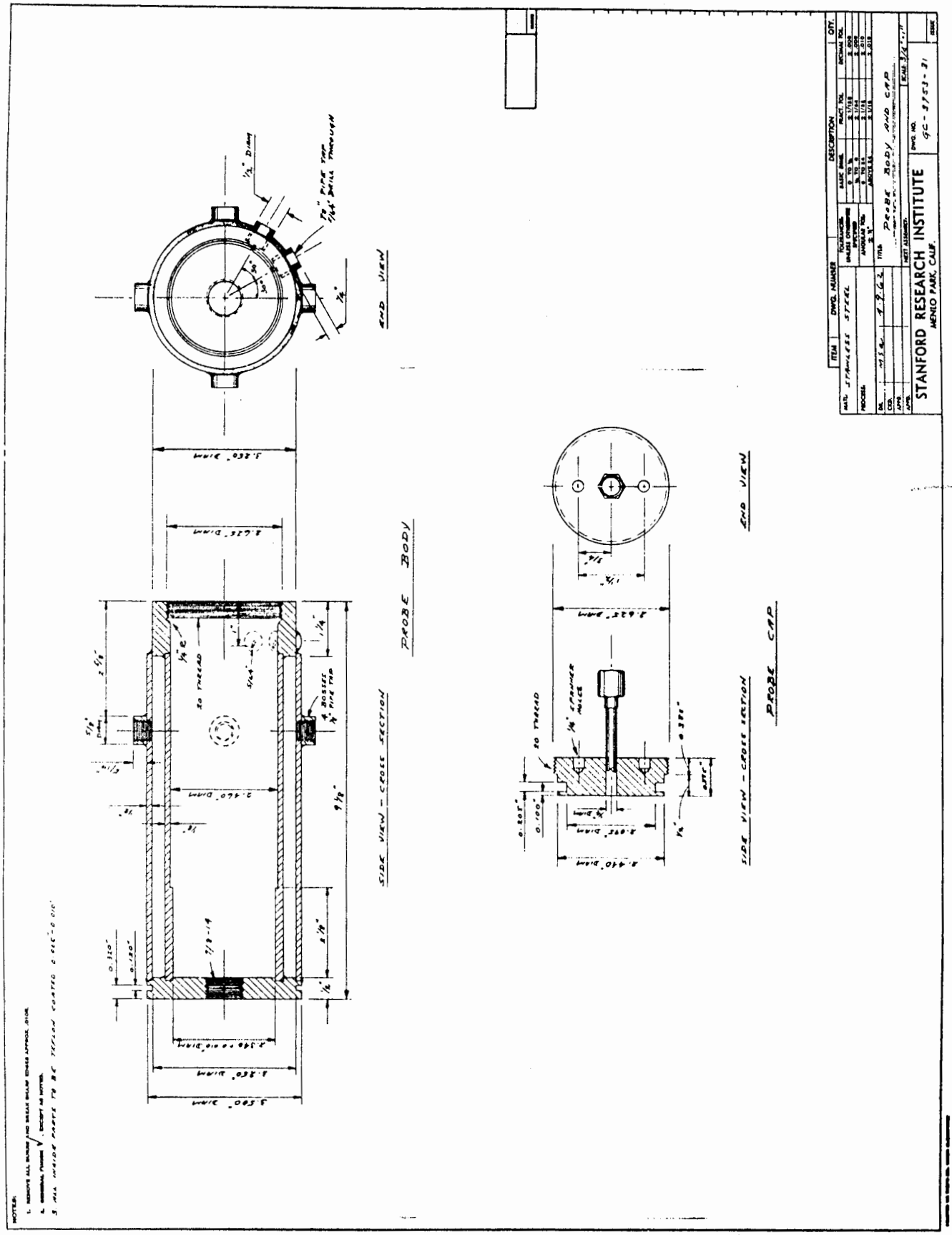

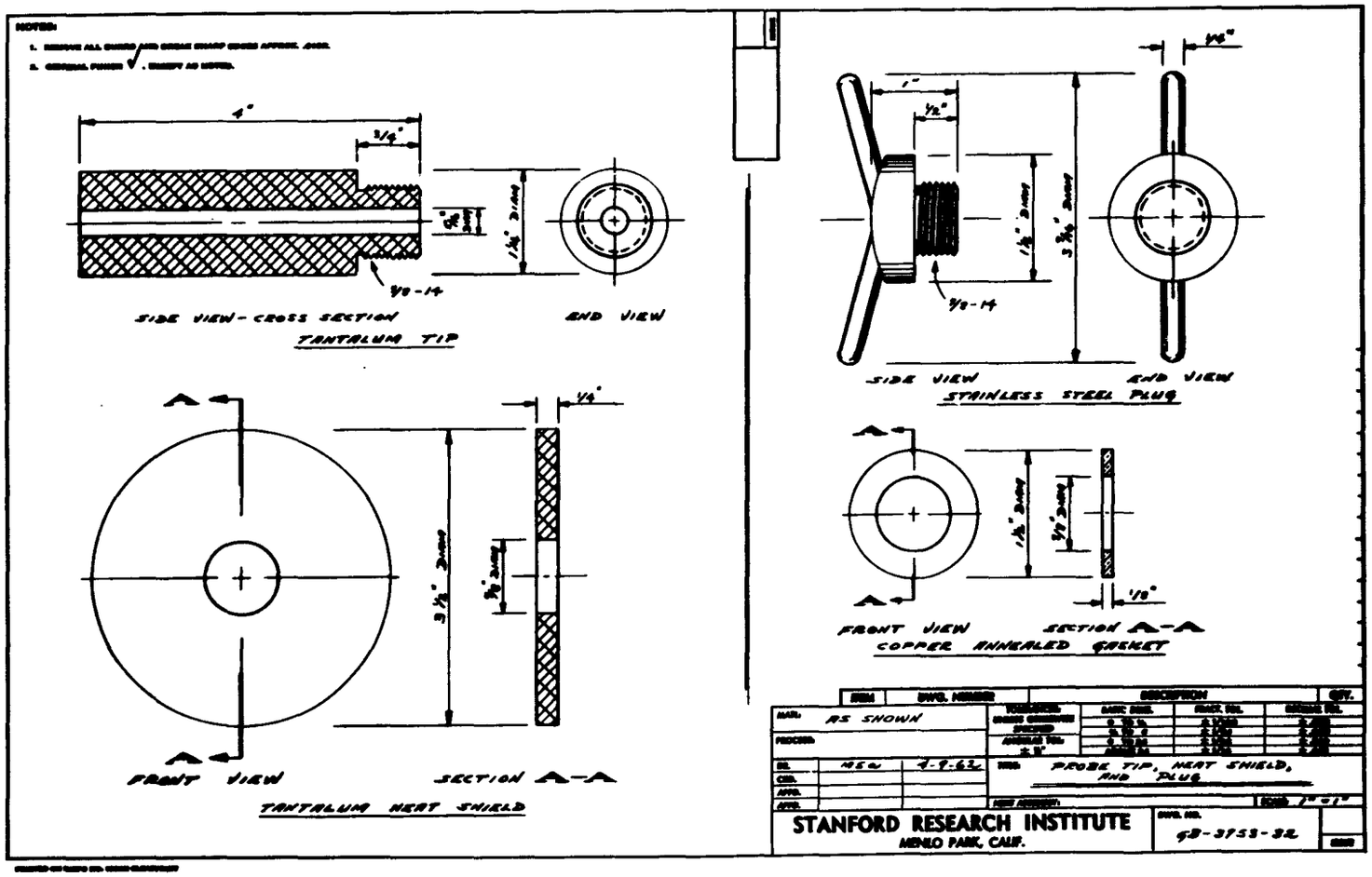
4"
3/4"
5/8" DIAM
1 1/4" DIAM
5/8-14
SIDE VIEW - CROSS SECTION
END VIEW
TANTALUM TIP
1/4"
3 1/8" DIAM
3/8" DIAM
FRONT VIEW
SECTION A-A
TANTALUM HEAT SHIELD
1"
1/2"
1 1/4" DIAM
3 3/8" DIAM
5/8-14
SIDE VIEW
END VIEW
STAINLESS STEEL PLUG
1 1/8" DIAM
1/2" DIAM
1/8"
FRONT VIEW
SECTION A-A
COPPER ANNEALED GASKET
ITEM
DWG. NUMBER
DESCRIPTION
QTY.
MATL: AS SHOWN
PROCESS
DR. MSM 4-9-62
CHK.
APPD.
APPD.
PROBE TIP, HEAT SHIELD, AND PLUG
SCALE 1" = 1"
STANFORD RESEARCH INSTITUTE
MENLO PARK, CALIF.
DWG. NO. SB-3753-32

NOTES:

1. REMOVE ALL BURRS AND BREAK SHARP EDGES APPROX. .010R.
2. GENERAL FINISH √, EXCEPT AS NOTED.

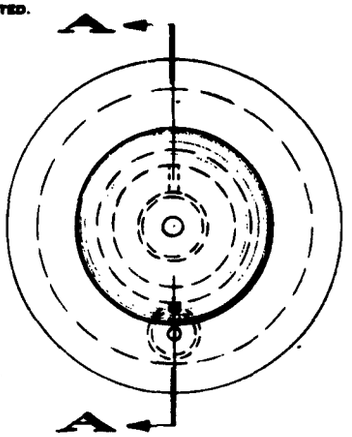

END VIEW

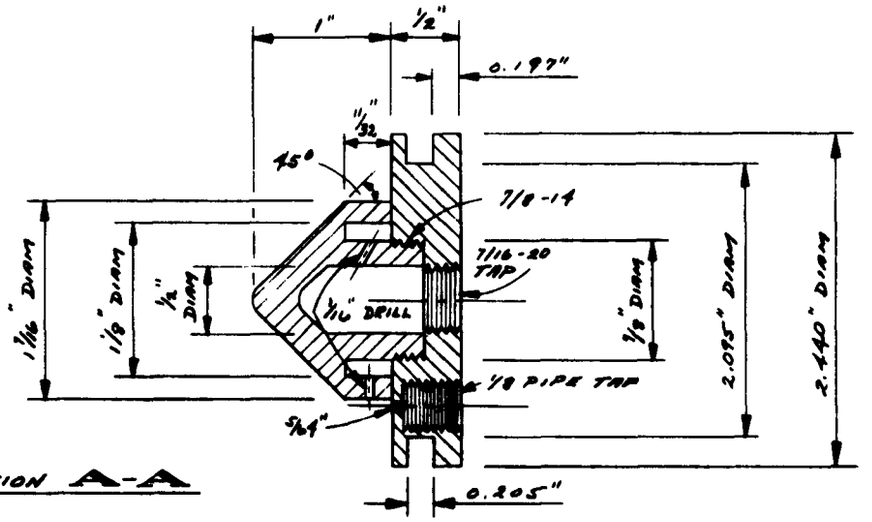

SECTION A-A

ITEM	DWG. NUMBER	DESCRIPTION	QTY.

MATL: STAINLESS STEEL

PROCESS:

DR.	MSW	9-9-62
CKD.		
APPD.		
APPD.		

TOLERANCES UNLESS OTHERWISE SPECIFIED	BASIC DIMS.	FRACT. TOL.	DECIMAL TOL.
ANGULAR TOL: ± 1°	0 TO ½	± 1/128	± .008
	½ TO 6	± 1/64	± .016
	6 TO 24	± 1/32	± .031
	ABOVE 24	± 1/16	± .062

TITLE: PARTICLE DEFLECTOR FOR PROBE

NEXT ASSEMBLY:

SCALE: 1" = 1"

STANFORD RESEARCH INSTITUTE
MENLO PARK, CALIF.

DWG. NO. GA-3753-33

ISSUE

PRINTED ON DIEPO NO. 1000H CLEARPRINT

NOTES:

1. REMOVE ALL BURRS AND BREAK SHARP EDGES APPROX. .010R.
2. GENERAL FINISH ✓, EXCEPT AS NOTED.

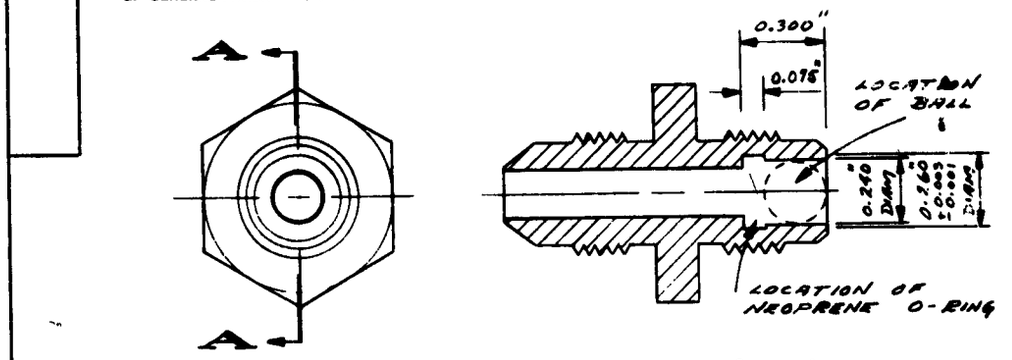

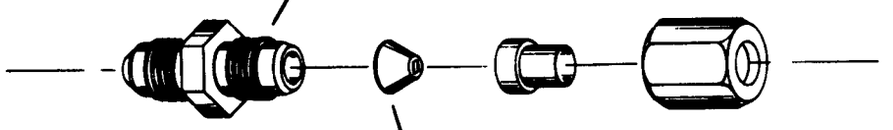

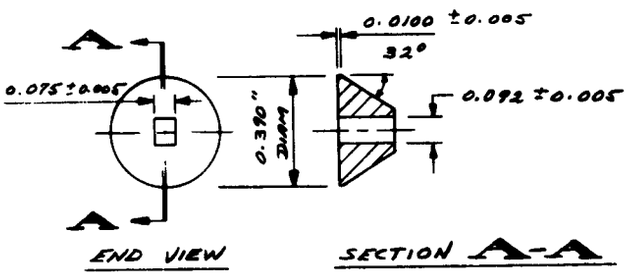

ITEM	DWG. NUMBER	DESCRIPTION	QTY.

MATL: STAINLESS STEEL

PROCESS:

TOLERANCES UNLESS OTHERWISE SPECIFIED: ANGULAR TOL: ± ½°

BASIC DIMS.	FRACT. TOL.	DECIMAL TOL.
0 TO ½	± 1/128	± .008
½ TO 6	± 1/64	± .008
6 TO 24	± 1/32	± .010
ABOVE 24	± 1/16	± .015

DR.	MSA	1 9 62
CKD.		
APPD.		
APPD.		

TITLE: CHECK VALVE UNIT

NEXT ASSEMBLY: SCALE: 2" = 1"

STANFORD RESEARCH INSTITUTE
MENLO PARK, CALIF.

DWG. NO. GA-3753-34

ISSUE

PRINTED ON DIEPO NO. 1000H CLEARPRINT

NOTES:

1. REMOVE ALL BURRS AND BREAK SHARP EDGES APPROX. .010R.
2. GENERAL FINISH √, EXCEPT AS NOTED.

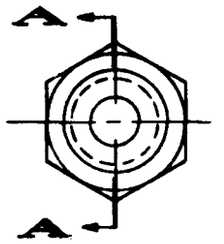

END VIEW

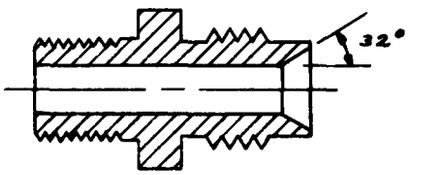

SECTION A-A

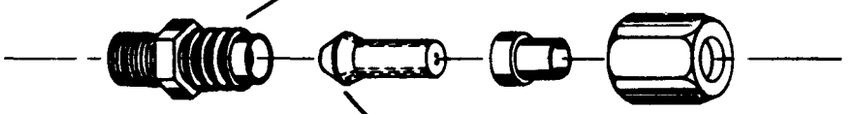

NO. 4 TUBE FITTING MODIFIED

4TX-SS SLEEVE

4BTL-SS NUT

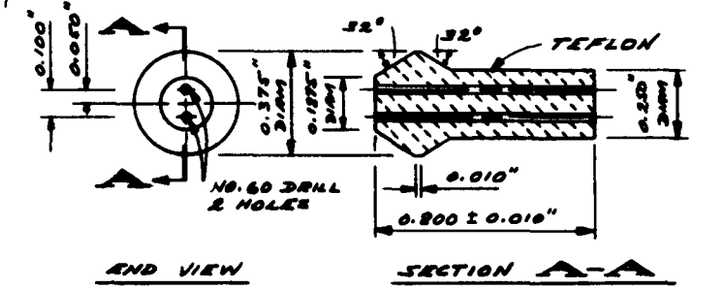

END VIEW

SECTION A-A

ITEM	DWG. NUMBER	DESCRIPTION	QTY.

MATL: STAINLESS STEEL OR AS INDICATED

PROCESS:

TOLERANCES UNLESS OTHERWISE SPECIFIED

ANGULAR TOL: ± ½°

BASIC DIMS.	FRACT. TOL.	DECIMAL TOL.
0 TO ¼	± 1/128	± .008
¼ TO 6	± 1/64	± .016
6 TO 24	± 1/32	± .032
ABOVE 24	± 1/16	± .062

DR.	MSO	4-9-62
CKD.		
APPD.		
APPD.		

TITLE: THERMOCOUPLE SEAL

NEXT ASSEMBLY:

SCALE: 2" = 1"

STANFORD RESEARCH INSTITUTE
MENLO PARK, CALIF.

DWG. NO. GA-3753-35

ISSUE

PRINTED ON DIEPO NO. 1000H CLEARPRINT

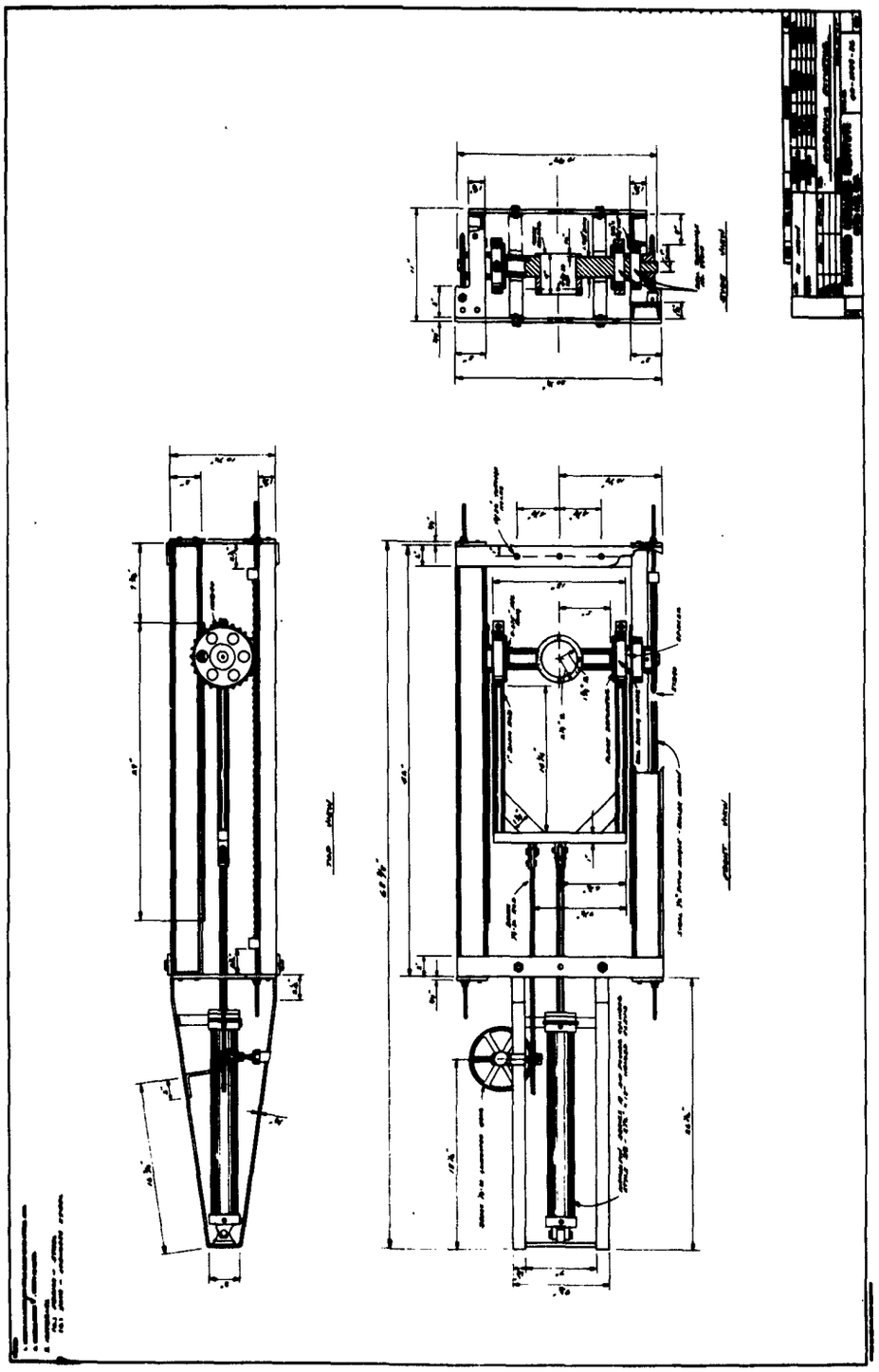

NOTES:

1. REMOVE ALL BURRS AND BREAK SHARP EDGES APPROX. .010R.
2. GENERAL FINISH √, EXCEPT AS NOTED.

TOP VIEW

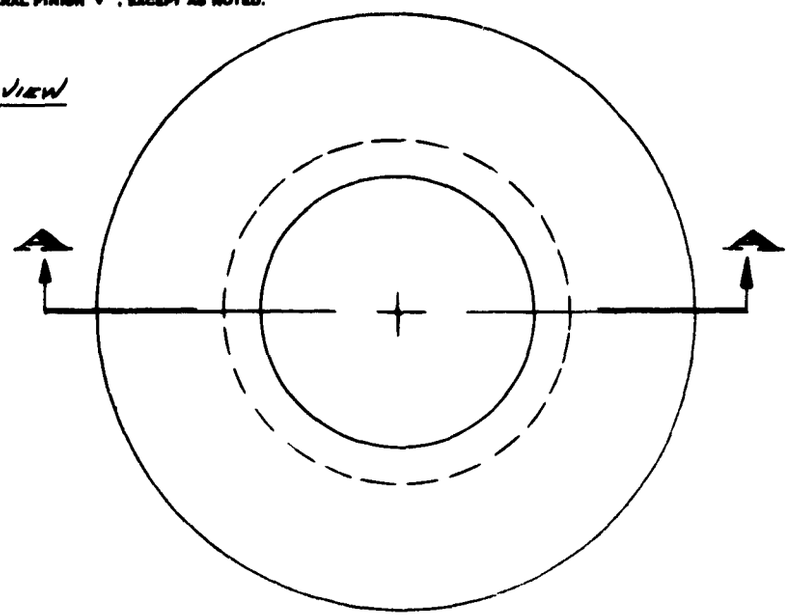

SECTION A-A

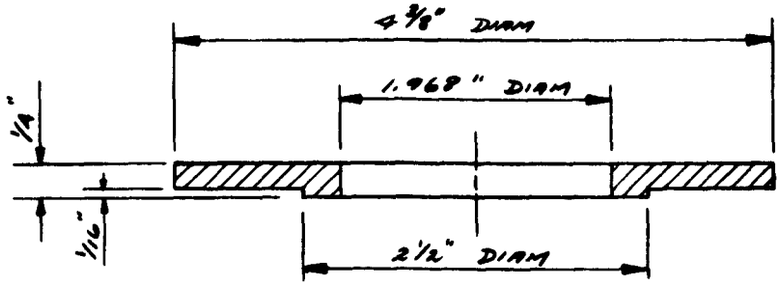

ITEM	DWG. NUMBER	DESCRIPTION	QTY.

MATL: STAINLESS STEEL

PROCESS:

DR.	MSR	4-9-62
CKD.		
APPD.		
APPD.		

TOLERANCES, UNLESS OTHERWISE SPECIFIED

ANGULAR TOL: ± ½°

BASIC DIMR.	FRACT. TOL.	DECIMAL TOL.
0 TO ½	± 1/128	± .008
½ TO 6	± 1/64	± .008
6 TO 24	± 1/32	± .010
ABOVE 24	± 1/16	± .015

TITLE: FLAME DEFLECTOR

NEXT ASSEMBLY:

SCALE: 1" = 1"

STANFORD RESEARCH INSTITUTE
MENLO PARK, CALIF.

DWG. NO. 9A-3753-37

ISSUE

PRINTED ON DIEPO NO. 1000H CLEARPRINT

NOTES:

1. REMOVE ALL BURRS AND BREAK SHARP EDGES APPROX. .010R.
2. GENERAL FINISH √. EXCEPT AS NOTED.

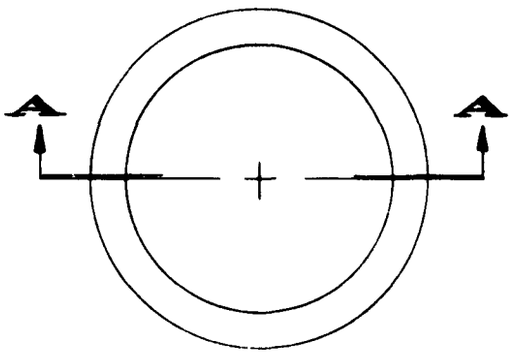

TOP VIEW

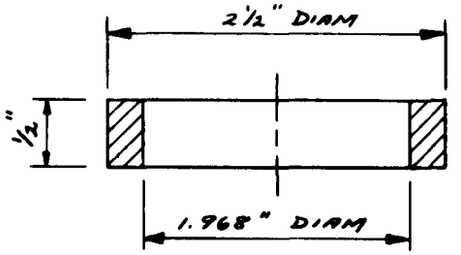

SECTION A-A

ITEM	DWG. NUMBER	DESCRIPTION	QTY.

MATL: STAINLESS STEEL

PROCESS:

TOLERANCES UNLESS OTHERWISE SPECIFIED

BASIC DIMS.	FRACT. TOL.	DECIMAL TOL.
0 TO ½	±1/128	±.008
½ TO 6	±1/64	±.008
6 TO 24	±1/32	±.010
ABOVE 24	±1/16	±.015

ANGULAR TOL: ± 1°

DR.	MSA	4-9-62
CKD.		
APPD.		
APPD.		

TITLE: SPACER

NEXT ASSEMBLY:

SCALE: 1" = 1"

STANFORD RESEARCH INSTITUTE
MENLO PARK, CALIF.

DWG. NO. GM-3753-3P

ISSUE

PRINTED ON DIEPO NO. 1000H CLEARPRINT

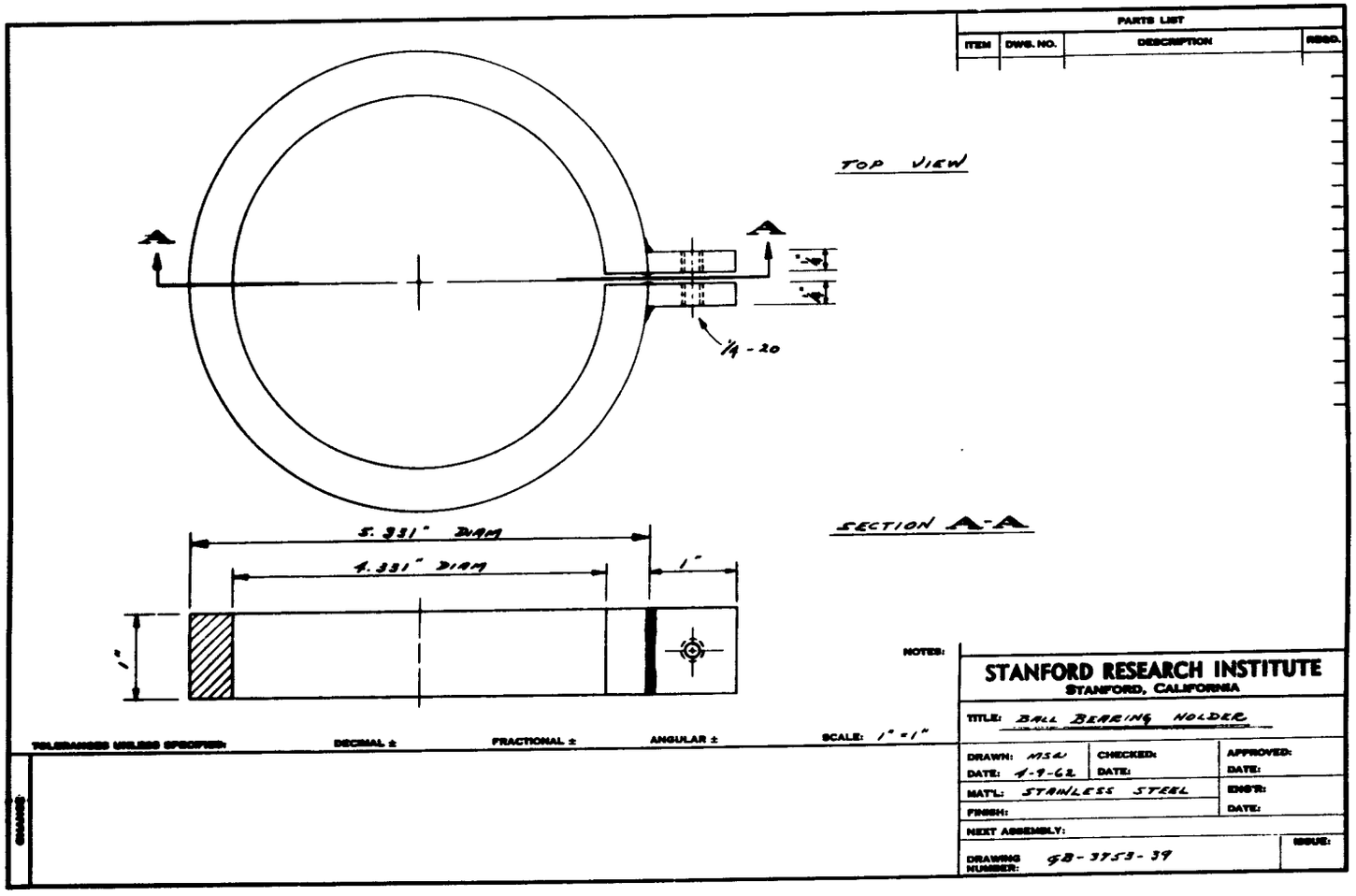
PARTS LIST
ITEM
DWG. NO.
DESCRIPTION
REQD.
TOP VIEW
A
A
1/4 - 20
SECTION A-A
5.331" DIAM
4.331" DIAM
1"
1"
NOTES:
STANFORD RESEARCH INSTITUTE
STANFORD, CALIFORNIA
TITLE: BALL BEARING HOLDER
DRAWN: MSU
DATE: 4-9-62
CHECKED:
DATE:
APPROVED:
DATE:
MAT'L: STAINLESS STEEL
FINISH:
ENG'R:
DATE:
NEXT ASSEMBLY:
DRAWING NUMBER: SB-3753-39
ISSUE:
TOLERANCES UNLESS SPECIFIED:
DECIMAL ±
FRACTIONAL ±
ANGULAR ±
SCALE: 1" = 1"
CHANGE:

STANFORD
RESEARCH
INSTITUTE

MENLO PARK
CALIFORNIA

Regional Offices and Laboratories

Southern California Laboratories
820 Mission Street
South Pasadena, California

Washington Office
808 17th Street, N.W.
Washington 5, D.C.

New York Office
270 Park Avenue, Room 1770
New York 17, New York

Detroit Office
The Stevens Building
1025 East Maple Road
Birmingham, Michigan

European Office
Pelikanstrasse 37
Zurich 1, Switzerland

Japan Office
911 Iino Building
22, 2-chome, Uchisaiwai-cho, Chiyoda-ku
Tokyo, Japan

Representatives

Honolulu, Hawaii
Finance Factors Building
195 South King Street
Honolulu, Hawaii

London, England
19 Upper Brook Street
London, W. 1, England

Milan, Italy
Via Macedonio Melloni 40
Milano, Italy

London, Ontario, Canada
P.O. Box 782
London, Ontario, Canada